Supporting Information for
"$PM_{2.5}$ Data Reliability, Consistency and Air Quality Assessment in Five Chinese Cities"

Xuan Liang[1], Shuo Li[2], Shuyi Zhang[1], Hui Huang[3,4], and Song Xi Chen[1,3,5]

[1]Guanghua School of Management, Peking University, Beijing, China.

[2]Department of Statistics, Tianjin University of Finance and Economics, Tianjin, China.

[3]Center for Statistical Science, Peking University, Beijing, China.

[4]Department of Probability and Statistics, Peking University, Beijing, China.

[5]Department of Statistics, Iowa State University of Science and Technology, Ames, Iowa, USA.

Contents

Introduction

In the Supporting Information, we provide more data analysis results, technical details about the weather-adjustment and variance calculations, and more information on the geographical conditions, energy consumptions and economic status of the five cities.

Corresponding author: Song Xi Chen, `csx@gsm.pku.edu.cn`

Corresponding author: Hui Huang, `huanghui@math.pku.edu.cn`

Text S1. Information about Different $\mathbf{PM_{2.5}}$ Concentration Ranges

In this section, we provide the analysis results about the different $PM_{2.5}$ concentration Ranges for each city. We have shown evidences for data consistency between the US posts and MEP sites in the main text. Hence the episodes information are based on the US posts alone.

The time range of our study for Beijing was from January 2010 to December 2014, and those for Shanghai, Guangzhou, Chengdu and Shenyang were from January 2012 to December 2014, April 2012 to March 2015, July 2013 to June 2015 and June 2013 to May 2015, respectively. Figure S1 displays box plots on the duration of three $PM_{2.5}$ concentration ranges (“$PM_{2.5} \leq 35\mu g/m^3$”, “$PM_{2.5} > 35\mu g/m^3$” and “$PM_{2.5} > 150\mu g/m^3$”) (panel a) and the percentages of time under four $PM_{2.5}$ concentration ranges (“$PM_{2.5} \leq 35\mu g/m^3$”, “$35\mu g/m^3 < PM_{2.5} \leq 75\mu g/m^3$” , “$75\mu g/m^3 < PM_{2.5} \leq 150\mu g/m^3$, “$PM_{2.5} > 150\mu g/m^3$”) (panel b). These figures provide overviews on the severity and seasonal pattern of $PM_{2.5}$ pollution in the five cities without taking into account of the weather conditions.

If we use the duration and the percentage of time under the “$PM_{2.5} > 35\mu g/m^3$” and “$PM_{2.5} > 150\mu g/m^3$” ranges as the measures, Figure S1 shows that Chengdu and Beijing were the worst among the five cities. If we use the percentage of good quality air (“$PM_{2.5} \leq 35\mu g/m^3$”) as the measure, Chengdu (12%) was the worst followed by Shenyang (22%); Beijing (24%) ranked the third. If we use the percentage of “$PM_{2.5} > 150\mu g/m^3$” as the measure, Beijing (22%) was the worst followed by Shenyang (11%) and Chengdu (9%). It is alarming to see that even in Guangzhou and Shanghai, the two best cities in terms of the duration statistics, at most 37% of the time had the acceptable quality air (“$PM_{2.5} \leq 35\mu g/m^3$”), and the average duration of pollution episodes (“$PM_{2.5} > 35\mu g/m^3$”) was around 2 days. These imply how much improvement are needed in order to clean up the air pollution in China. More results of the duration statistics are given in Table S1 and Table S2.

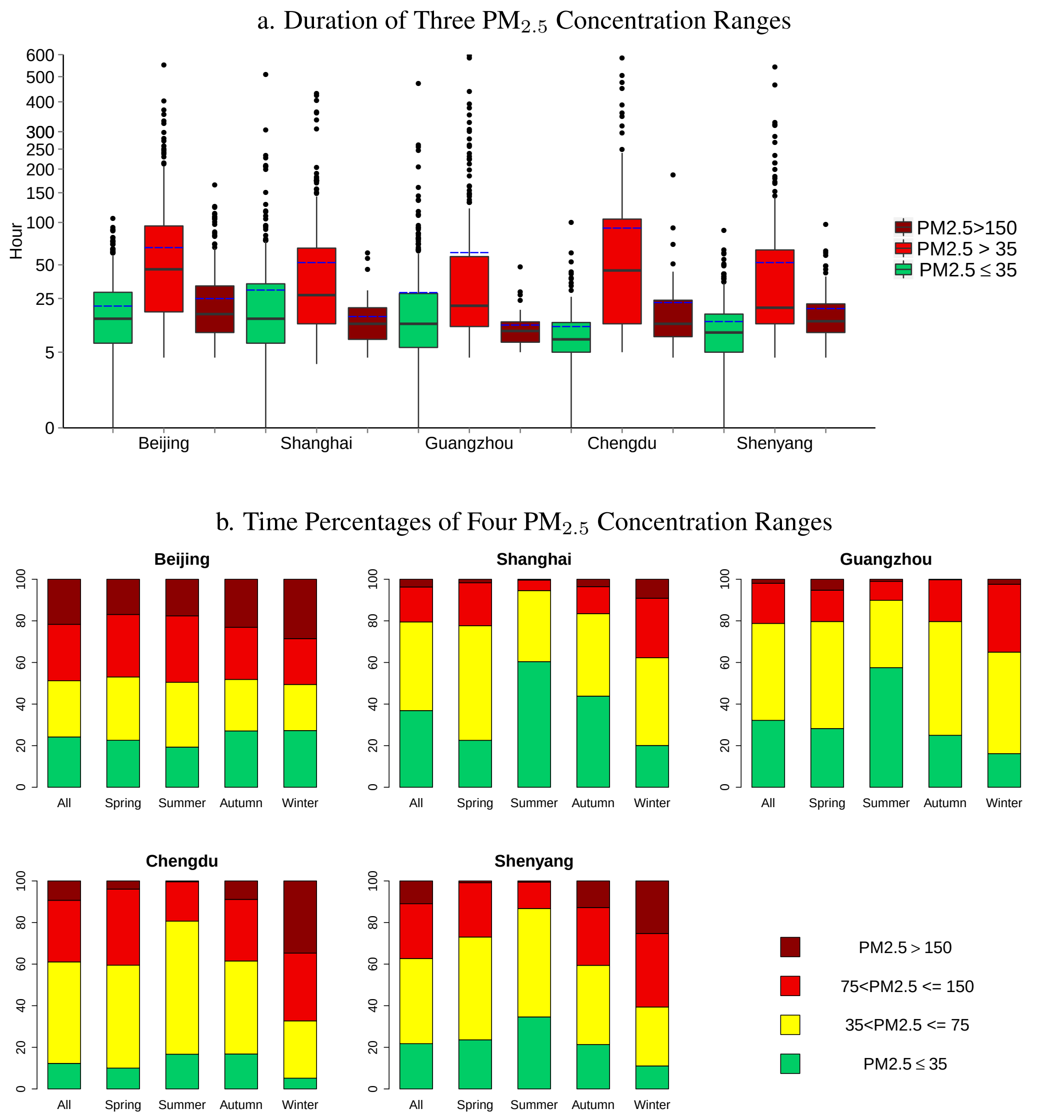

Figure S1. a. Boxplots on the duration under three $PM_{2.5}$ concentration ranges; b. Distributions of time in percentages (%) of four $PM_{2.5}$ concentration ranges in the five cities.

Table S1. Three $PM_{2.5}$ concentration ranges in the US posts of the five mega-cities. The minimum (Min), 25% percentile, Median, Mean, 75% percentile and maximum (Max) of the duration length (in hours) and the standard deviations (numbers in the parenthesis) for each range are reported.

(a) Beijing

	n	Min	25% percentile	Median	Mean	75% percentile	Max	Percentage
$PM_{2.5} \leq 35\mu g/m^3$	438	0	7 (0.58)	15 (0.91)	21 (0.94)	29(1.82)	106	24%
$PM_{2.5} > 35\mu g/m^3$	425	4	18 (2.32)	46 (3.14)	68 (3.34)	95 (5.48)	551	76%
$PM_{2.5} > 150\mu g/m^3$	329	4	10 (0.72)	17 (0.91)	25 (1.31)	33 (2.81)	165	22%

(b) Shanghai

	n	Min	25% percentile	Median	Mean	75% percentile	Max	Percentage
$PM_{2.5} \leq 35\mu g/m^3$	299	0	7 (1.86)	15 (2.06)	30 (2.81)	34 (2.40)	509	37%
$PM_{2.5} > 35\mu g/m^3$	298	3	13 (1.2)	27 (2.35)	52 (3.89)	67 (5.92)	432	63%
$PM_{2.5} > 150\mu g/m^3$	57	4	8 (1.24)	13 (1.52)	16 (1.54)	20 (2.13)	62	4%

(c) Guangzhou

	n	Min	25% percentile	Median	Mean	75% percentile	Max	Percentage
$PM_{2.5} \leq 35\mu g/m^3$	247	0	6 (1.96)	13 (2.17)	29 (3.10)	28 (2.31)	472	32%
$PM_{2.5} > 35\mu g/m^3$	240	4	12 (1.47)	22 (1.91)	63 (6.98)	58 (6.85)	737	68%
$PM_{2.5} > 150\mu g/m^3$	34	5	7 (1.58)	11 (1.73)	13 (1.49)	14 (1.73)	48	2%

(d) Chengdu

	n	Min	25% percentile	Median	Mean	75% percentile	Max	Percentage
$PM_{2.5} \leq 35\mu g/m^3$	120	0	5 (1.01)	8 (1.14)	12 (1.25)	14 (1.26)	100	12%
$PM_{2.5} > 35\mu g/m^3$	112	5	13 (4.06)	46 (6.44)	92 (11.78)	107 (14.37)	610	88%
$PM_{2.5} > 150\mu g/m^3$	48	4	9 (3.94)	13 (4.41)	23 (4.31)	24 (4.16)	187	9%

(e) Shenyang

	n	Min	25% percentile	Median	Mean	75% percentile	Max	Percentage
$PM_{2.5} \leq 35\mu g/m^3$	223	0	5 (0.67)	10 (0.81)	14 (0.91)	17 (1.22)	89	22%
$PM_{2.5} > 35\mu g/m^3$	215	4	13 (1.77)	20 (2.10)	52 (5.10)	65 (7.18)	542	78%
$PM_{2.5} > 150\mu g/m^3$	80	4	10 (1.39)	14 (1.58)	20 (1.81)	22 (2.17)	97	11%

Table S2. Annual baseline and seasonal percentages for the pollution states of $PM_{2.5}$ from the US posts of the five mega-cities.

(a) Beijing

	Annual Baseline	Spring	Summer	Autumn	Winter
$PM_{2.5} \leq 35\mu g/m^3$	24%	23%	19%	27%	27%
$35\mu g/m^3 < PM_{2.5} \leq 150\mu g/m^3$	54%	60%	66%	51%	45%
$PM_{2.5} > 150\mu g/m^3$	22%	17%	15%	22%	28%

(b) Shanghai

	Annual Baseline	Spring	Summer	Autumn	Winter
$PM_{2.5} \leq 35\mu g/m^3$	37%	23%	60%	44%	20%
$35\mu g/m^3 < PM_{2.5} \leq 150\mu g/m^3$	59%	75%	40%	53%	71%
$PM_{2.5} > 150\mu g/m^3$	4%	2%	0%	3%	9%

(c) Guangzhou

	Annual Baseline	Spring	Summer	Autumn	Winter
$PM_{2.5} \leq 35\mu g/m^3$	32%	28%	57%	25%	16%
$35\mu g/m^3 < PM_{2.5} \leq 150\mu g/m^3$	66%	67%	42%	75%	82%
$PM_{2.5} > 150\mu g/m^3$	2%	5%	1%	0%	2%

(d) Chengdu

	Annual Baseline	Spring	Summer	Autumn	Winter
$PM_{2.5} \leq 35\mu g/m^3$	12%	10%	17%	17%	5%
$35\mu g/m^3 < PM_{2.5} \leq 150\mu g/m^3$	79%	86%	82%	78%	74%
$PM_{2.5} > 150\mu g/m^3$	9%	4%	1%	5%	21%

(e) Shenyang

	Annual Baseline	Spring	Summer	Autumn	Winter
$PM_{2.5} \leq 35\mu g/m^3$	22%	24%	35%	21%	11%
$35\mu g/m^3 < PM_{2.5} \leq 150\mu g/m^3$	66%	70%	62%	61%	63%
$PM_{2.5} > 150\mu g/m^3$	12%	6%	3%	18%	26%

Text S2. Meteorological Impacts

In this section, we investigate the influence of wind and precipitation on the $PM_{2.5}$ concentrations for the five cities.

S2.1 Wind

We first demonstrate our method for combing the winds and then discuss their influences for each city.

The weather data have 16 wind directions plus Calm and Variable (CV). CV means that either there is no clearly established wind direction or when the wind speed is less than 0.5 meter per second (0.5m/s). As a total of 17 wind directions would be too many for statistical analysis, we combine wind stronger than 0.5m/s into four broad categories: North-West (NW), North-East (NE), South-East (SE) and South-West (SW). For each city, we first allocate the directions of WNW, NW, NNW to NW; NNE, NE, ENE to NE; ESE, SE, SSE to SE, and SSW, SW, WSW to SW, respectively. Then, we consider how to classify the four main wind directions N, E, S, W to the two neighboring categories; for example, N to NW or NE. This leads to a total of 16 assignments of the main wind directions.

Let Y_t be the $PM_{2.5}$ reading at time t, X_t be the vector of the covariates: Dew Point, Temperature, Pressure, Cumulative Wind Power and Cumulative Precipitation. Denote W_t as the wind direction indicators such that $W_t = 1, 2, 3, 4, 5$ for CV, NW, NE, SE and SW, respectively. Cumulative Wind Power (C) is an integral of wind speed over time under one wind direction. Whenever W_t changes, the cumulation resets to zero and starts to cumulate again. Cumulative Precipitation is similarly defined.

The classification of the main wind directions is based on the fitting performance to the auto-regressive partially linear model:

$$Y_t = \beta Y_{t-1} + g(X_t, W_t) + \eta_t. \tag{S.1}$$

Liang et al. [2015] has technical details on the model fitting. Since the weather conditions have seasonal variations, we fit the model (S.1) for each season (three months) under each of the 16 combinations of the main wind directions, and obtain their root mean square errors (RMSE). We average the RMSEs within the four seasons to get an annual averaged RMSE. We choose a combination with the minimum averaged RMSE. The chosen combinations for the five cities are shown in Table S3.

Table S3. Classifications of Wind Directions (clockwise) in the Five Cities.

Category	Beijing	Shanghai	Guangdong	Chengdu	Shenyang
NW	W to N	W to NNW	WNW to N	WNW to N	WNW to N
NE	NNE to ENE	N to E	NNE to E	NNE to E	NNE to ENE
SE	E to S	ESE to SSE	ESE to SSE	ESE to SSE	E to SSE
SW	SSW to WSW	S to WSW	S to W	S to W	S to W

Seasonal wind patterns for each city are provided in Figure S2. Beijing has more northerly winds in autumn and winter, especially the northwesterly ones. In spring and summer, southerly wind dominates. It is more likely to have easterly wind in Shanghai. Especially in spring and summer, the ratio of SE increases a lot with stronger force, while in winter and autumn, the northerly wind has larger percentage than other two seasons. In the five cities, Guangzhou and Chengdu have milder winds in all seasons. The most frequent winds for Guangzhou and Shenyang are northwesterly and southerly, respectively. In Guangzhou, northwesterly wind is much more prevailing in autumn and winter and easterly wind is with larger proportions in spring and autumn. Similar to Beijing, Shenyang has more northwesterly wind in autumn and winter and more southwesterly wind in spring and summer. Situated in the basin, Chengdu has milder wind and the seasonal differences about the wind directions are less.

a. Beijing

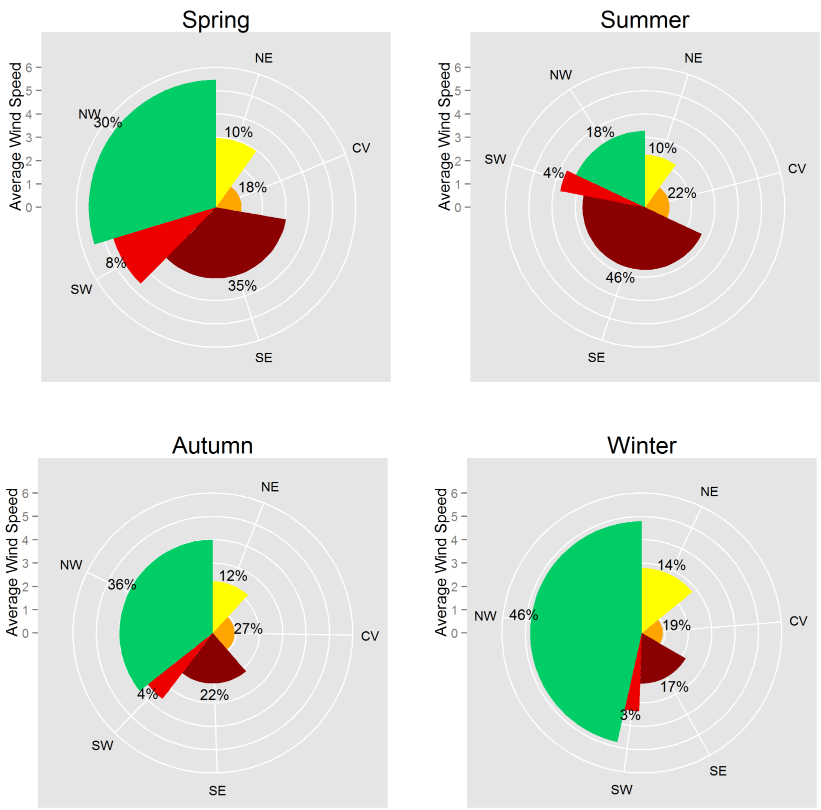

b. Shanghai

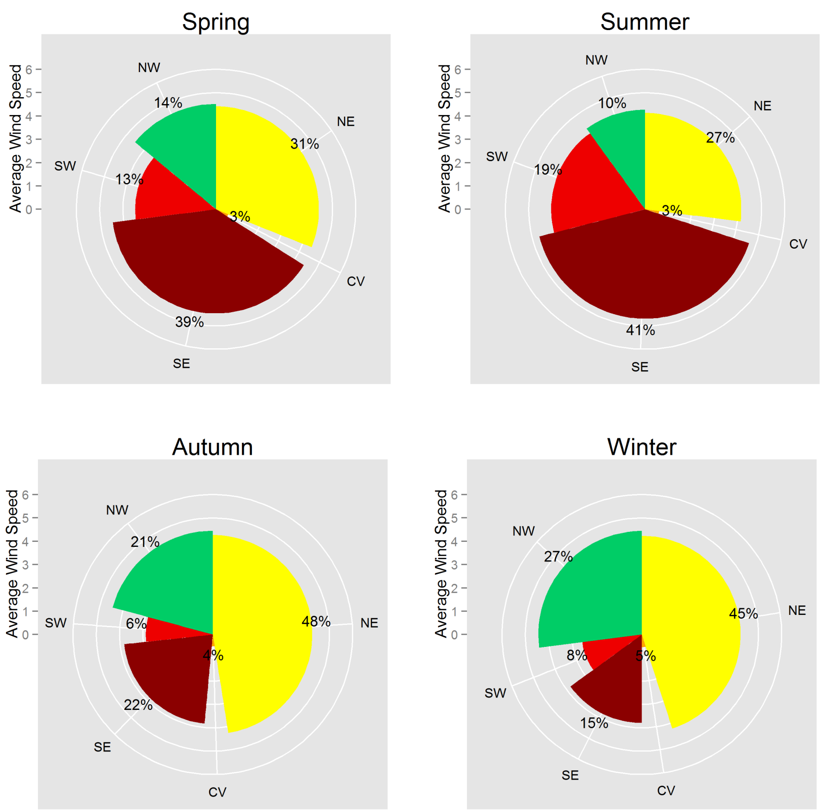

c. Guangzhou

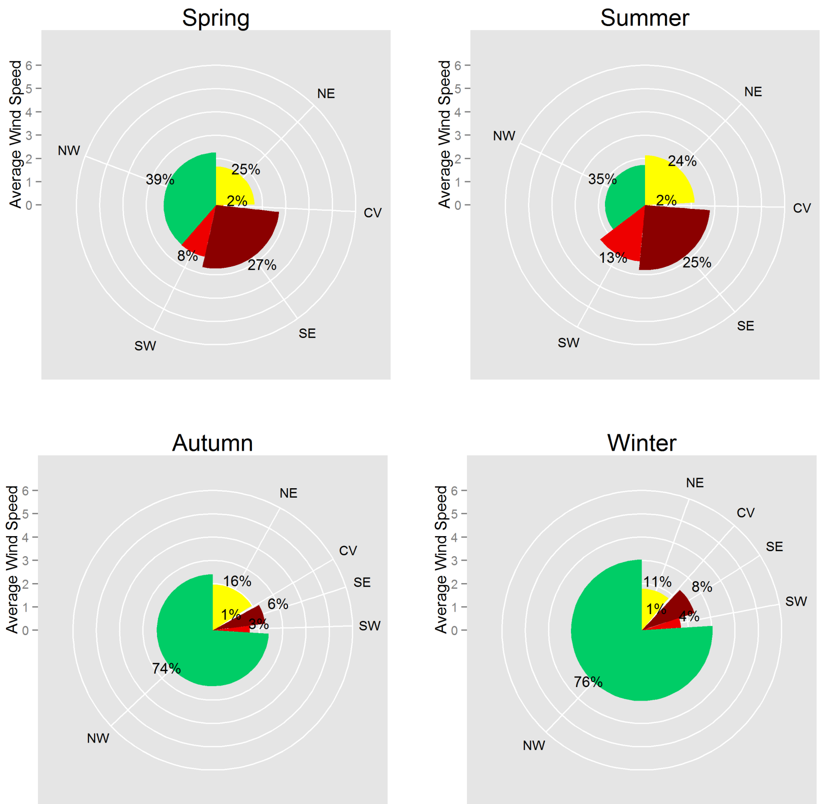

d. Chengdu

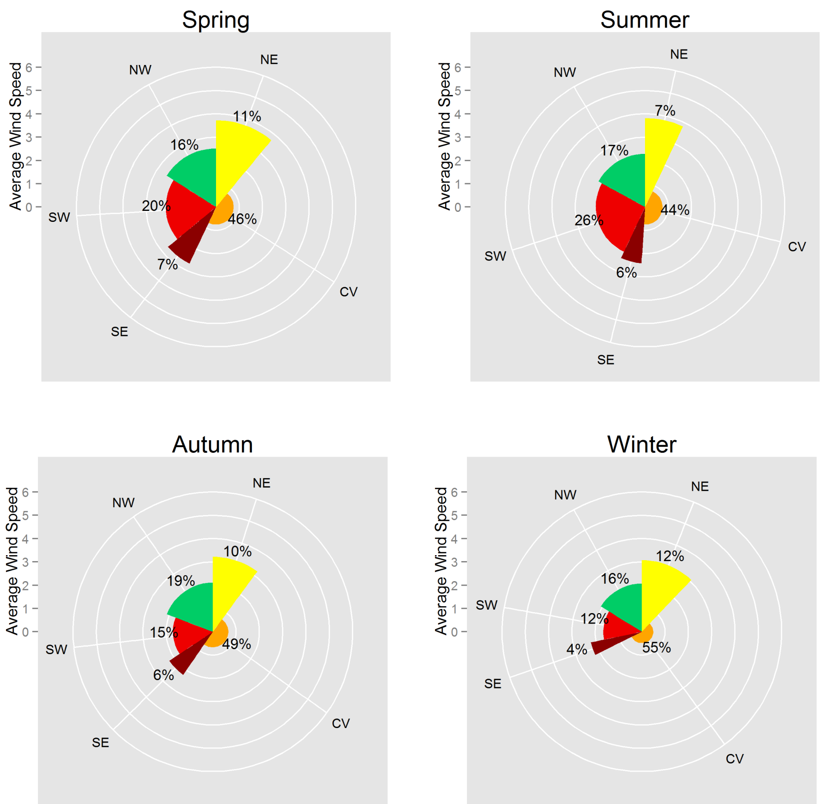

e. Shenyang

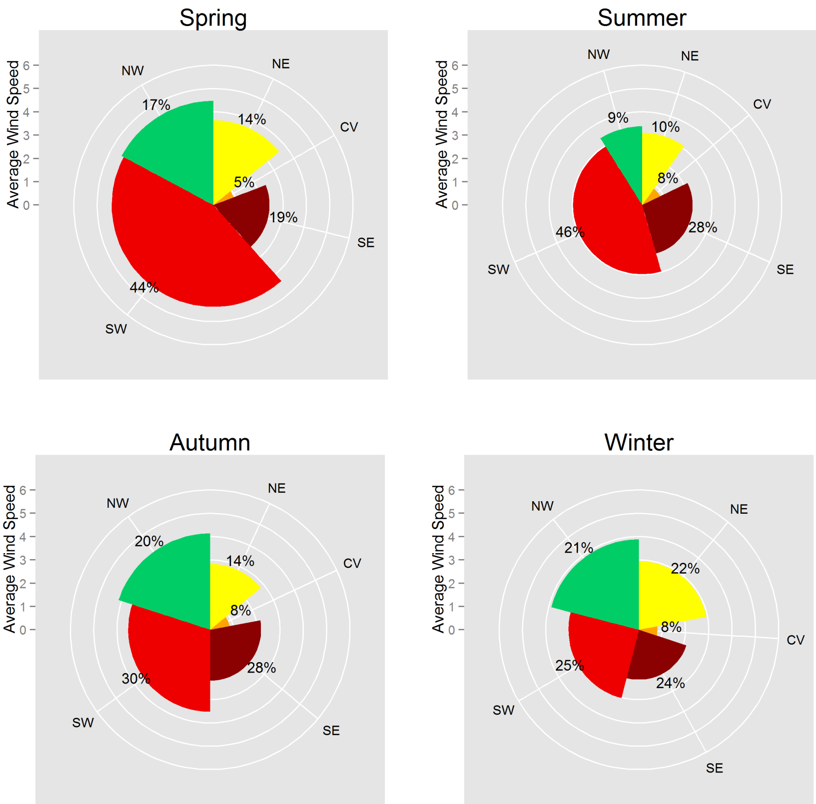

Figure S2. Distributions of wind directions (via the width of angles) and average speeds (via the length of radius) in the five cities in four seasons: Spring, Summer, Autumn, Winter.

To gain insight on the impact of the wind on the $PM_{2.5}$, we display in Figure S3 radar plots on the distributions of the wind directions (NW, NE, SW, SE and CV) and their respective average speeds under different states of $PM_{2.5}$ concentration ranges: "$PM_{2.5} \leq 35\mu g/m^3$", "$PM_{2.5} > 35\mu g/m^3$", "$PM_{2.5} > 150\mu g/m^3$", the beginning and the ending periods of the pollution episodes and the baseline level. Here we define a beginning (ending) period as a five-hour-interval centered at the hour that the $PM_{2.5}$ density first surpasses (drops below) $35\mu g/m^3$.

Figure S3 shows that the beneficial wind direction that has the ability to reduce $PM_{2.5}$ level are, respectively, northerly winds (NW and NE) in Beijing and Chengdu; easterly winds (NE and SE) in Shanghai; SE winds in Guangzhou, NW in Shenyang since in "$PM_{2.5} \leq 35\mu g/m^3$" range these winds account for more proportions compared with those in baseline for each city. It is clear that the "$PM_{2.5} > 150\mu g/m^3$" range is largely associated with high percentage of CV wind and low wind speed in all cities, and the "$PM_{2.5} \leq 35\mu g/m^3$" range is strongly associated with strongly wind and lower proportion of CV. Figure S3 also suggests that the pollution inducing wind directions are respectively, southerly (SE and SW) in Beijing, westerly (SW and NW) in Shanghai, NW in Guangzhou, easterly (NE and SE) in Shenyang, and large proportion of CV in Chengdu by more frequency in the "$PM_{2.5} > 35\mu g/m^3$" and "$PM_{2.5} > 150\mu g/m^3$" ranges. The beneficial wind directions tend to be related to rural places with low industry loads, which is largely coincided with our discussion about the geographic conditions for each city in Section S6. On the other hand, those $PM_{2.5}$-inducing directions tend to be associated with regions of industries around.

a. Beijing

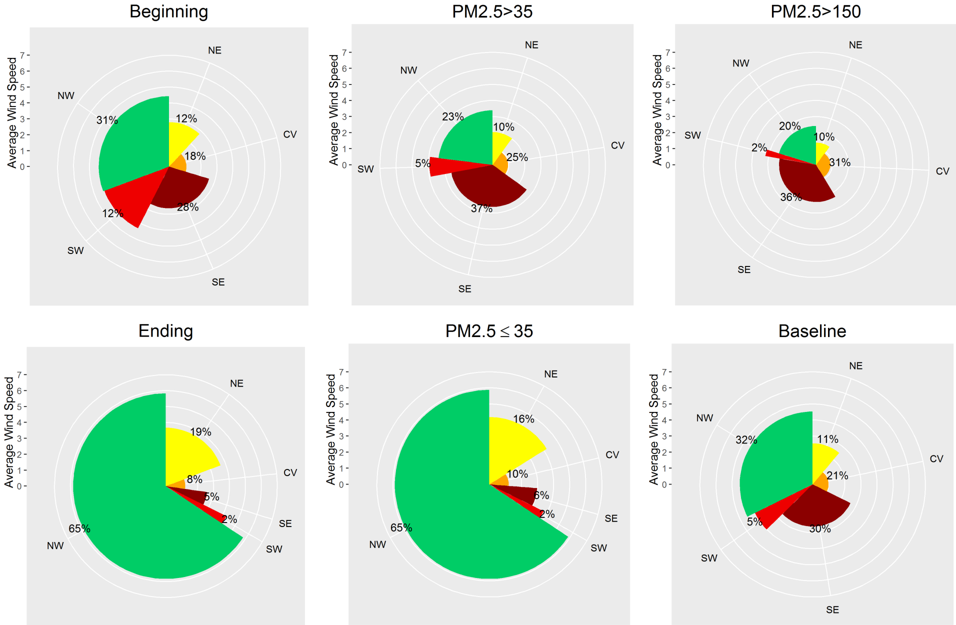

b. Shanghai

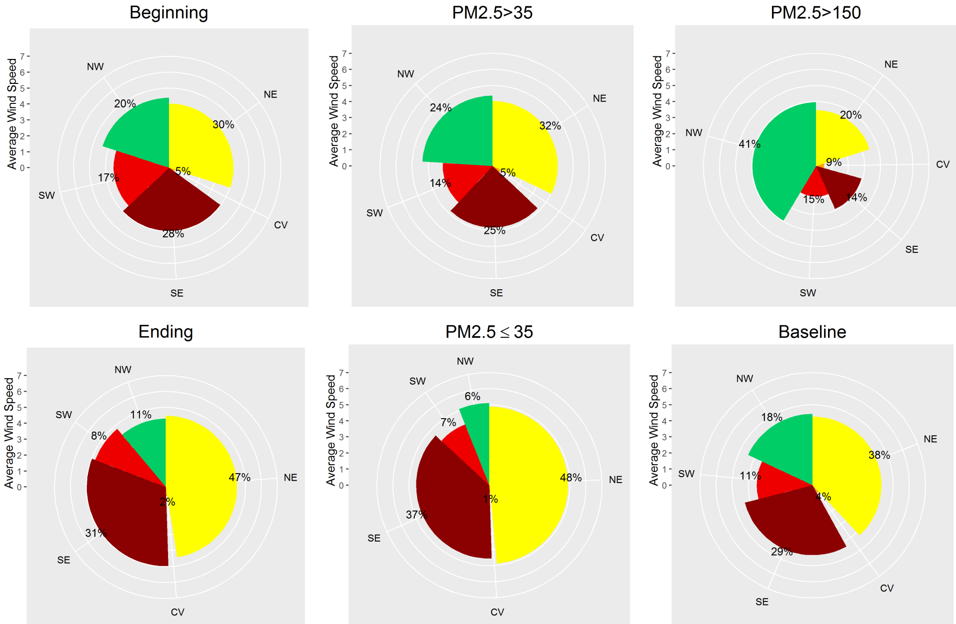

c. Guangzhou

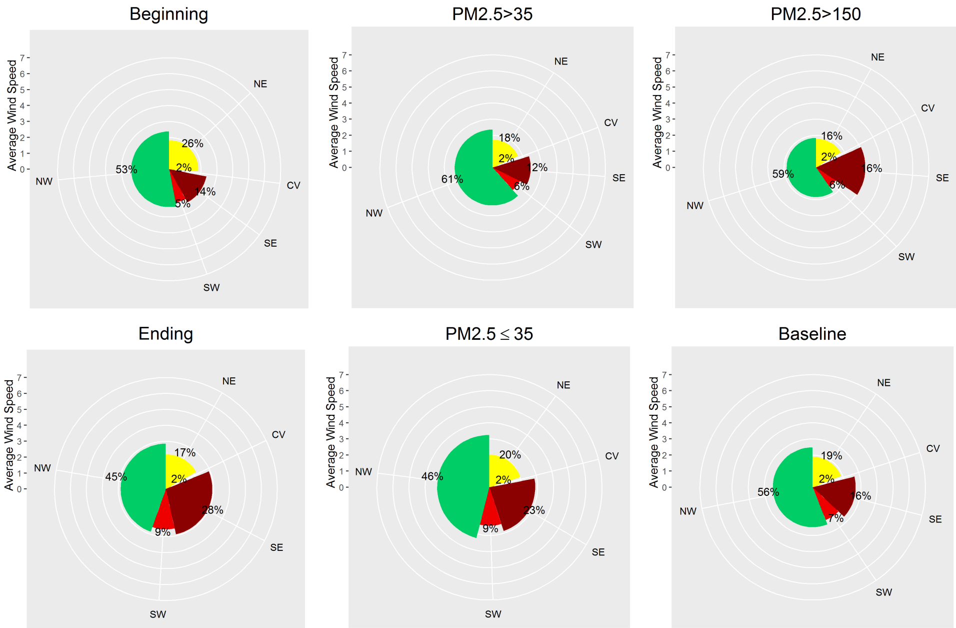

d. Chengdu

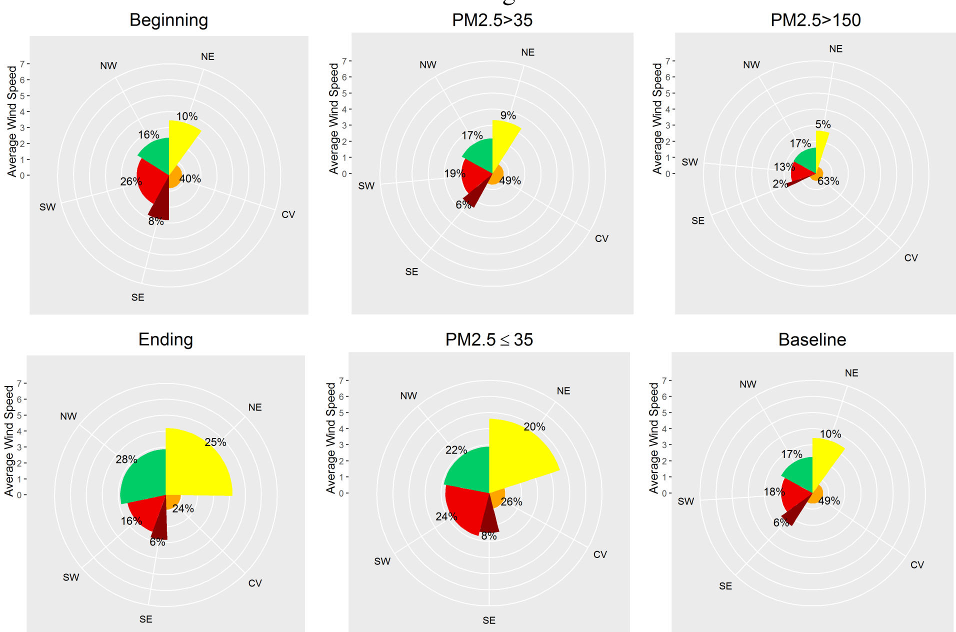

e. Shenyang

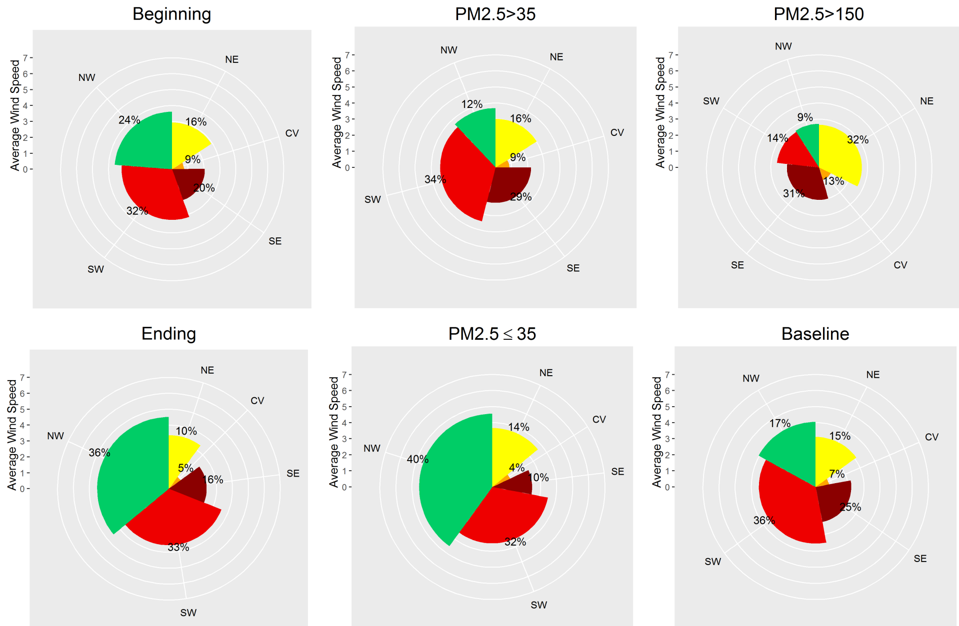

Figure S3. Distributions of wind directions (via width of the angles) and average speeds (via length of the radius) in the five cities under the six $PM_{2.5}$ concentration ranges: Beginning/Ending, "$PM_{2.5} > 35\mu g/m^3$", "$PM_{2.5} > 150\mu g/m^3$", "$PM_{2.5} \leq 35\mu g/m^3$" and the baseline.

S2.2 Precipitation

Precipitation in the forms of rain and snow may reduce the $PM_{2.5}$ concentration. We fit a nonlinear regression model between the $PM_{2.5}$ data with the cumulative precipitation (R) data. Figure S4 shows the relationship between $PM_{2.5}$ and non-zero cumulative precipitation for the five cities. The red lines are the fitted nonparametric regression functions. As the cumulation gets larger, the trend in $PM_{2.5}$ significantly decreases for all cities. In humid places such as Shanghai, Guangzhou and Chengdu, the cumulative precipitation is much larger than the dry places such as Beijing and Shenyang. Moreover, for all the five cities, the $PM_{2.5}$ readings go below the $35\mu g/m^3$ level when the cumulative precipitation is higher than 50mm.

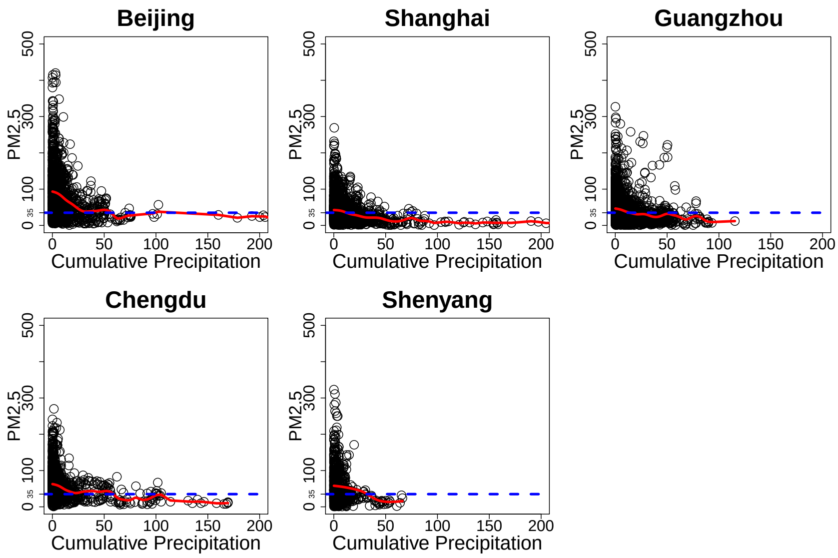

Figure S4. Scatter plots of $PM_{2.5}$ vs non-zero cumulative precipitation (Unit: mm). The red lines are fitted nonparametric regression functions.

Furthermore, we study the proportions of cumulative precipitations in the three states of PM$_{2.5}$ levels in each city. Figure S5 (panel a) reveals that the "PM$_{2.5} > 150\mu g/m^3$" range has the largest proportion with "$R = 0$" while the "PM$_{2.5} \leq 35\mu g/m^3$" has the least percentage of "$R = 0$", which is consistent with the scatter plots for all the cities. Conditioning on positive cumulative precipitation, Figure S5 (panel b) shows that the proportion of "$0 < R < 10$" is the largest in the "PM$_{2.5} > 150\mu g/m^3$" range while when PM$_{2.5}$ is less than $35\mu g/m^3$", the proportion of "$R \geq 10$" is the largest among the three PM$_{2.5}$ concentration ranges. Thus, a high level of cumulative precipitation can reduce the PM$_{2.5}$ concentration.

a.

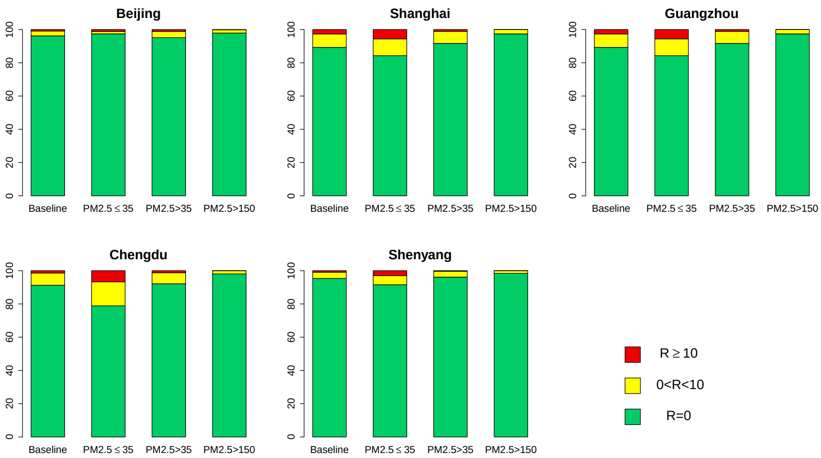

b.

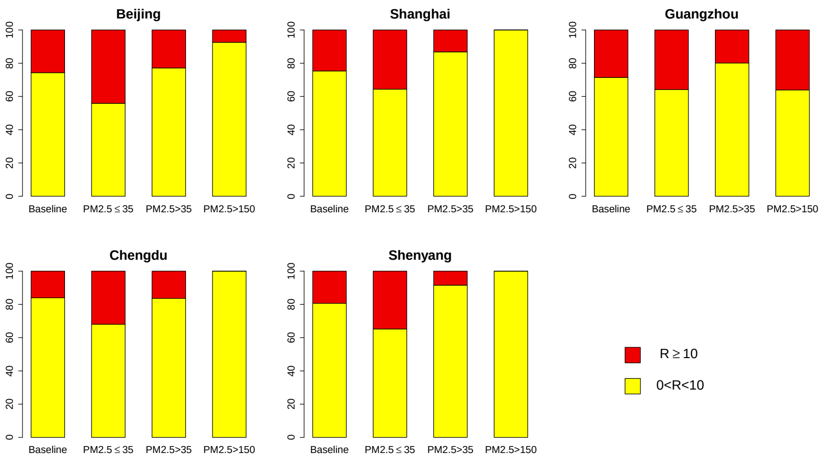

Figure S5. Relation of PM$_{2.5}$ and cumulative precipitation (R) (Unit: mm). a. Proportions (%) of 3 levels of R under different ranges of PM$_{2.5}$ concentration in the five cities. b. Proportions (%) of 2 levels of R given positive precipitation under different ranges of PM$_{2.5}$ concentration in the five cities.

Text S3. Adjusting the Weather Conditions

S3.1 Estimation of the Meteorologically Adjusted Mean

Denote W_{ijt} as the combined wind direction defined in Table S3 such that $W_{ijt} = 1, 2, 3, 4, 5$ for CV, NW, NE, SE and SW, respectively. For Beijing, we merge SE and SW to S since the percentage of SW is rather small, which makes $W_{ijt} = 1, 2, 3, 4$ for CV, NW, NE and S.

According to the main text, we know that the weather-adjusted average $PM_{2.5}$ at site s can be written as

$$\mu^s_{ij} = \int m^s_{ij}(x, w) f_j(x, w) dx dw. \tag{S.2}$$

Substituting the meteorological data to (S.2) and taking average over all available years, we get the estimator of μ^s_{ij}

$$\hat{\mu}^s_{ij} = (\sum_{a=1}^{n} n_{aj})^{-1} \sum_{a=1}^{n} \sum_{t=1}^{n_{aj}} \hat{m}^s_{ij}(X_{ajt}, W_{ajt}), \tag{S.3}$$

once we get the estimator $\hat{m}^s_{ij}(x, w)$ by using the approach outlined in the main text.

In each city, we have S sites for $PM_{2.5}$ measurements and one site for the meteorological data. To combine these information, we take the average of the conditional mean functions

$$m_{ij}(x, w) \quad = \quad \frac{1}{S} \sum_{s=1}^{S} m^s_{ij}(x, w).$$

Substituting $m^s_{ij}(x, w)$ with $\hat{m}^s_{ij}$ at site s, we have

$$\hat{m}_{ij}(x, w) \quad = \quad \frac{1}{S} \sum_{s=1}^{S} \hat{m}^s_{ij}(x, w).$$

Replacing $\hat{m}^s_{ij}$ in (S.3) with $\hat{m}_{ij}$, we get the weather-adjusted average for each city:

$$\hat{\mu}_{ij} = (\sum_{a=1}^{n} n_{aj})^{-1} \sum_{a=1}^{n} \sum_{t=1}^{n_{ij}} \hat{m}_{ij}(X_{ajt}, W_{ajt}). \tag{S.4}$$

This estimator $\hat{\mu}_{ij}$ contains all the information from the S sites.

S3.2 Estimation of the Meteorologically Adjusted Percentiles

Similar to the weather-adjusted average in (S.2), we define the meteorologically adjusted distribution function of $PM_{2.5}$ for month j of year i at site s as

$$G^s_{ij}(y) \quad = \quad \int F^s_{ij}(y|x, w) f_j(x, w) dx dw,$$

where $F^s_{ij}(y|x,w) = E(I\left\{Y^s_{ijt} \leq y\right\}|X_{ijt} = x, W_{ijt} = w)$ is a conditional distribution at site s.

To estimate $G^s_{ij}(y)$, we replace $\hat{m}^s_{ij}(x,w)$ in (S.3) with $\hat{F}^s_{ij}(y|x,w) = \hat{F}^s_{ij0}(x_1,0,w)I(x_2 = 0) + \hat{F}^s_{ij+}(x_1,x_2,w)I(x_2 > 0)$ by kernel smoothing estimators:

$$
\begin{aligned}
\hat{F}^s_{ij0}(x_1,0,w) &= \frac{\sum_{t=1}^{n_{ij}} K(\frac{X_{ijt,1}-x_1}{h_1})I(X_{ijt,2}=0, W_{ijt}=w)G_{h_0}(Y^s_{ijt}-y)}{\sum_{t=1}^{n_{ij}} K(\frac{X_{ijt,1}-x_1}{h_1})I(X_{ijt,2}=0, W_{ijt}=w)} \\
\hat{F}^s_{ij+}(x_1,x_2,w) &= \frac{\sum_{t=1}^{n_{ij}} K_1(\frac{X_{ijt,1}-x_1}{h_1})K_2(\frac{X_{ijt,2}-x_2}{h_2})l(W_{ijt},w,\lambda)I(X_{ijt,2}>0)G_{h_0}(Y^s_{ijt}-y)}{\sum_{t=1}^{n_{ij}} K_1(\frac{X_{ijt,1}-x_1}{h_1})K_2(\frac{X_{ijt,2}-x_2}{h_2})l(W_{ijt},w,\lambda)I(X_{ijt,2}>0)},
\end{aligned}
$$

where $G_{h_0}(x) = \int_{-\infty}^{x/h_0} K(u)du$ [*Li and Racine*, 2007], $K(\cdot)$, $K_1(\cdot)$, $K_2(\cdot)$ and $l(\cdot)$ are defined same as those in $\hat{m}_{ij0}(\cdot)$ and $\hat{m}_{ij+}(\cdot)$ in the main text.

Then we have

$$
\hat{G}^s_{ij}(y) = \left\{\sum_{a=1}^{n} n_{aj}\right\}^{-1} \sum_{a=1}^{n}\sum_{t=1}^{n_{aj}} \hat{F}^s_{ij}(y|X_{ajt}, W_{ajt}).
$$

For any $q \in (0,1)$, the adjusted q-th percentile $\hat{\xi}^s(q)$ is estimated by the inverse function of $\hat{G}^s_{ij}(y)$.

To estimate an averaged weather-adjusted percentiles for S sites, we only need to estimate the averaged conditional distribution function by

$$
\hat{F}_{ij}(y|x,w) = \frac{1}{S}\sum_{s=1}^{S} \hat{F}^s_{ij}(y|x,w).
$$

Hence, we get

$$
\hat{G}_{ij}(y) = \left\{\sum_{a=1}^{n} n_{aj}\right\}^{-1} \sum_{a=1}^{n}\sum_{t=1}^{n_{aj}} \hat{F}_{ij}(y|X_{ajt}, W_{ajt}). \tag{S.5}
$$

According to (S.5), we can estimate $\hat{\xi}_{ij}(q)$ by the inverse function of $\hat{G}_{ij}(y)$.

S3.3 Block Bootstrap

In this subsection, we illustrate how to use a block bootstrap method to estimate the variance of the $\hat{\mu}_{ij}$ in (S.4). The variances of percentiles are obtained in a similar way.

For each city, denote $\{Z_{ijt} = (X_{ijt}, W_{ijt}, Y^1_{ijt}, \cdots, Y^S_{ijt}), t = 1, \cdots, T\}$ as the observed time series of weather conditions and $PM_{2.5}$ concentrations from S sites in month j and year i. Define $B_1 = (Z_{ij1}, \cdots, Z_{ijl}), \cdots, B_{T-l+1} = (Z_{ij,T-l+1}, \cdots, Z_{ij,T})$, $B_{T-l+2} = (Z_{ij,T-l+2}, \cdots, Z_{ij,T}, Z_{ij,1})$ $, \cdots, B_T = (Z_{ij,T}, Z_{ij,1}, \cdots, Z_{ij,l-1})$ as a series of moving blocks with length l. In our study, we choose $l = 12$ (hour). For the b-th replication, we independently resample $\frac{T}{l}$ blocks from $\{B_t, t = 1 \cdots T\}$ with equal probability and then combine them to get $\{(X_{ijt}^b, W_{ijt}^b), Y_{ijt}^{1,b}, \cdots, Y_{ijt}^{S,b}\}$ for month j, year i.

Then we reconstruct $PM_{2.5}$ series on the S sites as $\{\tilde{Y}_{ijt}^{1,b}, \cdots, \tilde{Y}_{ijt}^{S,b}\}$ according to

$$\tilde{Y}_{ijt}^{s,b} = \hat{m}_{ij}^{s,b}(X_{ijt}^b, W_{ijt}^b) + \hat{\epsilon}_{ijt}^{s,b} \quad \text{for} \quad s = 1, \cdots, S,$$

where $\hat{\epsilon}_{ijt}^{s,b}$ is the s-th element of $\hat{\epsilon}_{ijt}^b = (\hat{\epsilon}_{ijt}^{1,b}, \cdots, \hat{\epsilon}_{ijt}^{S,b})^\tau$ which follows a joint multi-normal distribution of dimension S with zero mean and covariance matrix $\hat{V}_{ij}(X_{ijt}^b, W_{ijt}^b)$. Here $\hat{V}_{ij}(x, w)$ captures the dependence among the sites. Let $\hat{V}_{ij}(x, w) = \hat{V}_{ij}(x_1, x_2, w)$ be a $S \times S$ diagonal matrix, whose s-th diagonal element is estimated by

$$\begin{aligned}
\hat{V}_{ij0}(x_1, 0, w)_{s\times s} &= \frac{\sum_{t=1}^{n_{ij}} K(\frac{X_{ijt,1}-x_1}{h_1}) I(X_{ijt,2} = 0, W_{ijt} = w)\hat{\epsilon}_{ijt,s}^2}{\sum_{t=1}^{n_{ij}} K(\frac{X_{ijt,1}-x_1}{h_1}) I(X_{ijt,2} = 0, W_{ijt} = w)}, \\
\hat{V}_{ij+}(x_1, x_2, w)_{s\times s} &= \frac{\sum_{t=1}^{n_{ij}} K(\frac{X_{ijt,1}-x_1}{h_1}) K(\frac{X_{ijt,2}-x_2}{h_2}) l(W_{ijt}, w, \lambda) I(X_{ijt,2} > 0)\hat{\epsilon}_{ijt,s}^2}{\sum_{t=1}^{n_{ij}} K(\frac{X_{ijt,1}-x_1}{h_1}) K(\frac{X_{ijt,2}-x_2}{h_2}) l(W_{ijt}, w, \lambda) I(X_{ijt,2} > 0)} \quad \text{for} \quad x_2 > 0,
\end{aligned}$$

where $\hat{\epsilon}_{ijt,s} = Y_{ijt}^s - \hat{m}_{ij}(X_{ijt}, W_{ijt})$.

Combining the reconstructed $PM_{2.5}$ series $\{\tilde{Y}_{ijt}^{1,b}, \cdots, \tilde{Y}_{ijt}^{S,b}\}$ with the weather data $\{(X_{ajt}^b, W_{ajt}^b)\}$, we re-estimate $\hat{m}_{ij}^{s,b}(x, w)$ at site s and get $\{\hat{m}_{ij}^{1,b}(x, w), \cdots, \hat{m}_{ij}^{S,b}(x, w)\}$. Then, a bootstrapped version of the adjusted average for the b-th replication is

$$\hat{\mu}_{ij}^b = (\sum_{a=1}^{n} n_{aj})^{-1} \sum_{a=1}^{n} \sum_{t=1}^{n_{aj}} \hat{m}_{ij}^b(X_{ajt}^b, W_{ajt}^b),$$

where $\hat{m}_{ij}^b(x, w) = S^{-1} \sum_{s=1}^{S} \hat{m}_{ij}^{s,b}(x, w)$. The bootstrapped variance of $\hat{\mu}_{ij}$ is then estimated by

$$\hat{\sigma}_{ij}^2 = (B-1)^{-1} \sum_{b=1}^{B} (\hat{\mu}_{ij}^b - \hat{\mu}_{ij})^2.$$

In our study, we use $B = 300$. A similar algorithm can be conducted to obtain the variance of $\hat{\xi}_{ij}(q)$.

Text S4. Consistent Adjustment between MEP sites and US Posts

In this section, we provide more assessment results for the five cities, and more evidences about the data consistency between the US posts and MEP sites.

Figure S6 and Figure S7 compare the adjusted monthly medians and 90th-percentiles of the US posts and nearby MEP data from January, 2013 to December, 2015. For all the five cities, strong consistency can be observed after we perform the adjustment of weather conditions, indicating that the US Embassy/Consulates and MEP sites tell the same story about the local emission levels.

Comparisons of yearly changes in medians and 90th-percentiles are also conducted. The results are shown in Figure S8. The similar patterns between the US Posts and MEP averages coincide with the monthly patterns, which is another proof of the data consistency. Moreover, the differences between two year's monthly percentiles quantify the extent of increase and reductions in emissions. Specifically, Figure S8 show that all the five cities except Shanghai have significantly lower $PM_{2.5}$ emissions in 2015 than 2013 and 2014. While by comparing 2014 with 2013 for all the 12 months, Beijing and Shenyang had no obvious improvement, but there are some reductions in the other three cities.

To further support the data consistency between the US posts and MEP readings, we report Pearson's correlation coefficients correlations of three air quality metrics: adjusted mean, median and 90th-percentiles. Suppose we have data $(X_1, ..., X_n)$ and $(Y_1, ..., Y_n)$, which are respectively simple random samples of random variables $\mathbf{X}$ and $\mathbf{Y}$. To check the linear correlation between $\mathbf{X}$ and $\mathbf{Y}$, a Pearson's correlation coefficient is defined by $r = \frac{\sum_{i=1}^{n}(X_i - \bar{X})(Y_i - \bar{Y})}{\sqrt{\sum_{i=1}^{n}(X_i - \bar{X})^2 \sum_{i=1}^{n}(Y_i - \bar{Y})^2}}$, where $\bar{X}$ and $\bar{Y}$ are sample averages. The correlations are reported in Table S4 and S5. Generally speaking, the three metrics are all highly correlated between the US posts and MEP results, which give a quantitative evidence of the data consistency.

Also, we have done the regression about the three air quality/ yearly changes metrics: adjusted mean, median and 90th-percentiles between MEP sites and US posts. The regression coefficients and R^2 are listed in Table S6. In all the five cities, the slopes are close to 1 and highly significant.

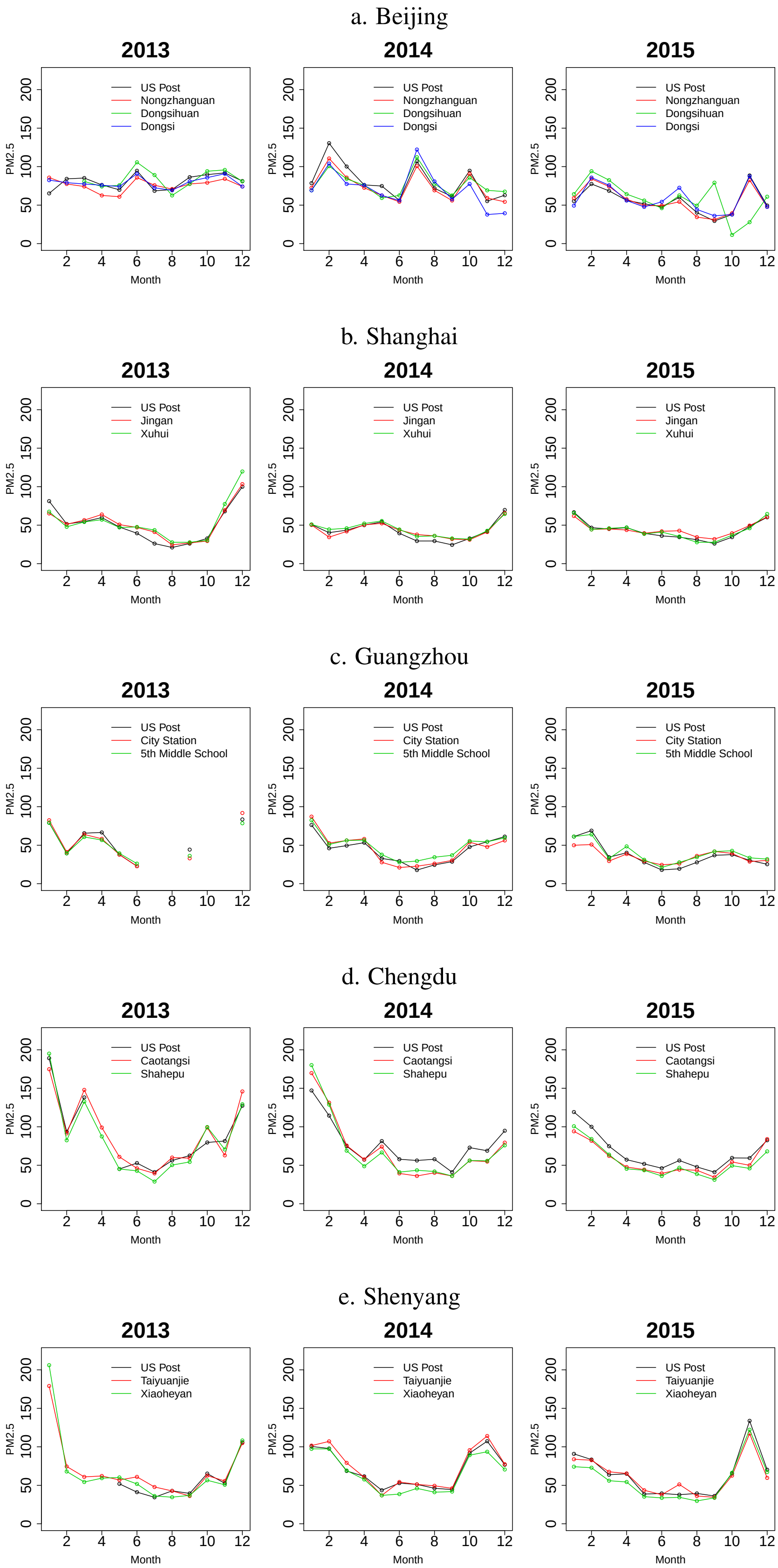

Figure S6. Meteorologically adjusted medians in the US posts and nearby MEP sites in the five cities from January 2013 to December 2015. The missed parts are due to lack of data.

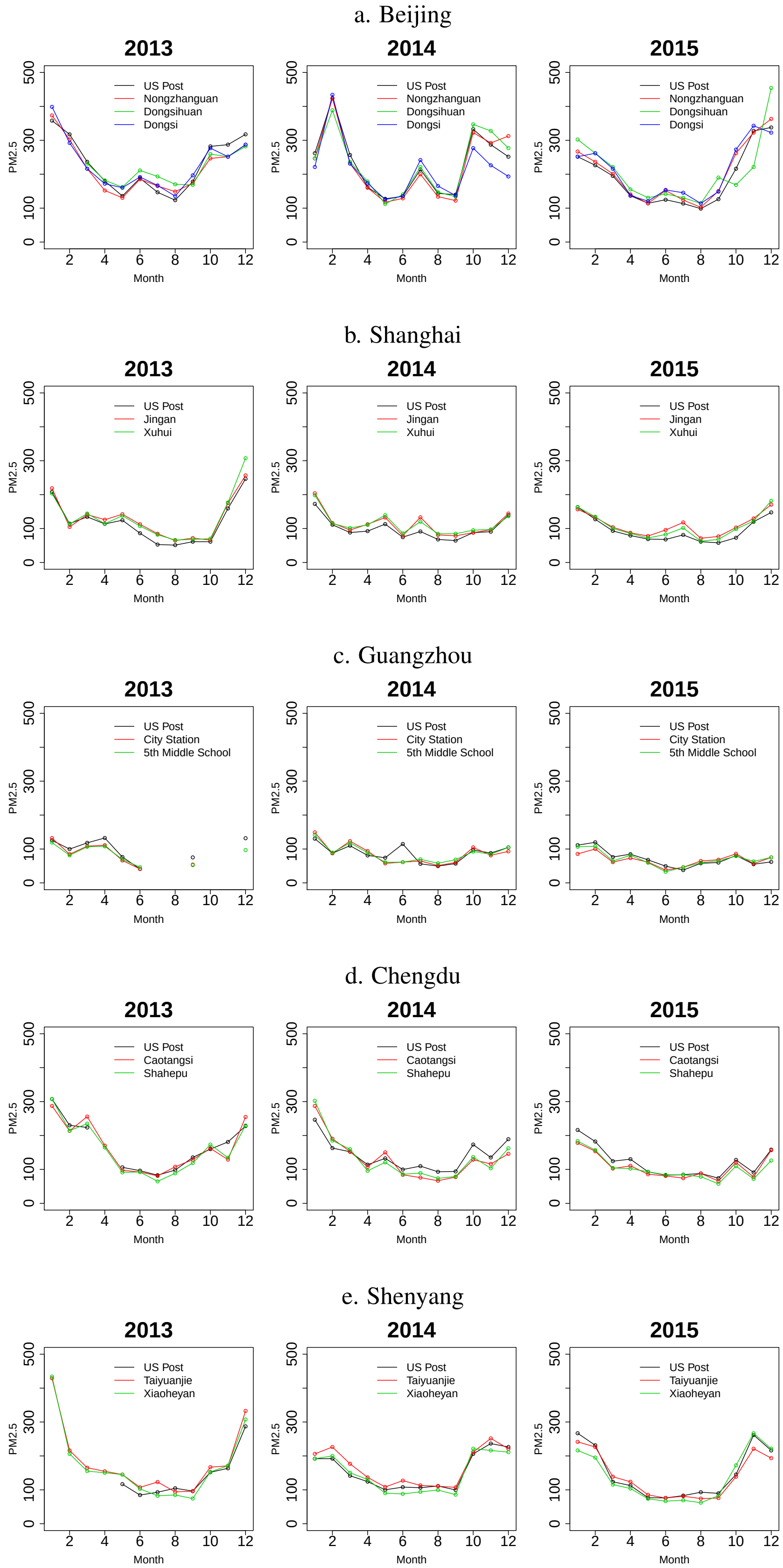

Figure S7. Meteorologically adjusted 90th-percentiles in US posts and nearby MEP sites in the five cities from January 2013 to December 2015. The missed parts are due to lack of data.

a. Beijing

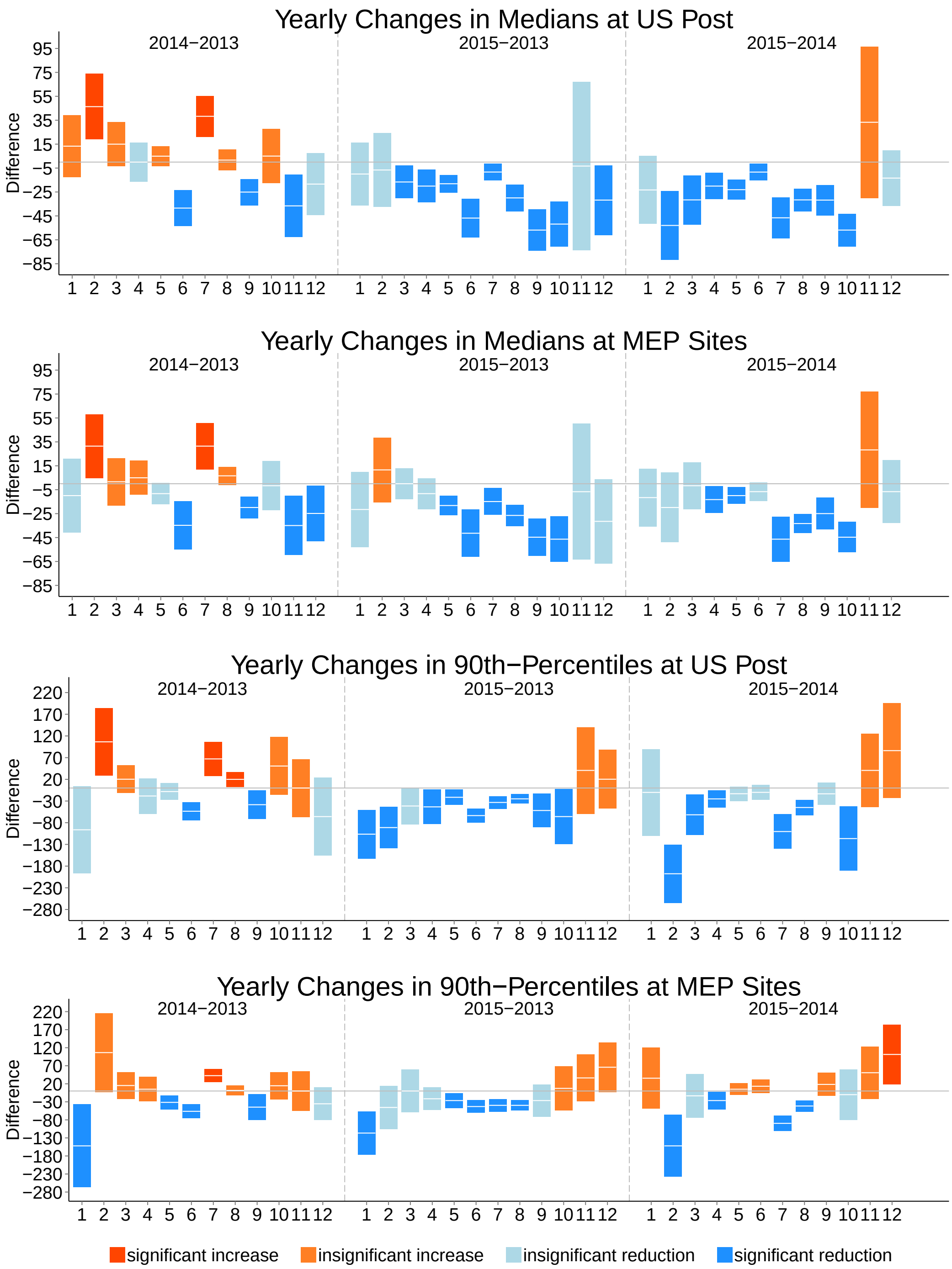
Yearly Changes in Medians at US Post
2014−2013
2015−2013
2015−2014
Difference
Yearly Changes in Medians at MEP Sites
Yearly Changes in 90th−Percentiles at US Post
Yearly Changes in 90th−Percentiles at MEP Sites
significant increase
insignificant increase
insignificant reduction
significant reduction

b. Shanghai

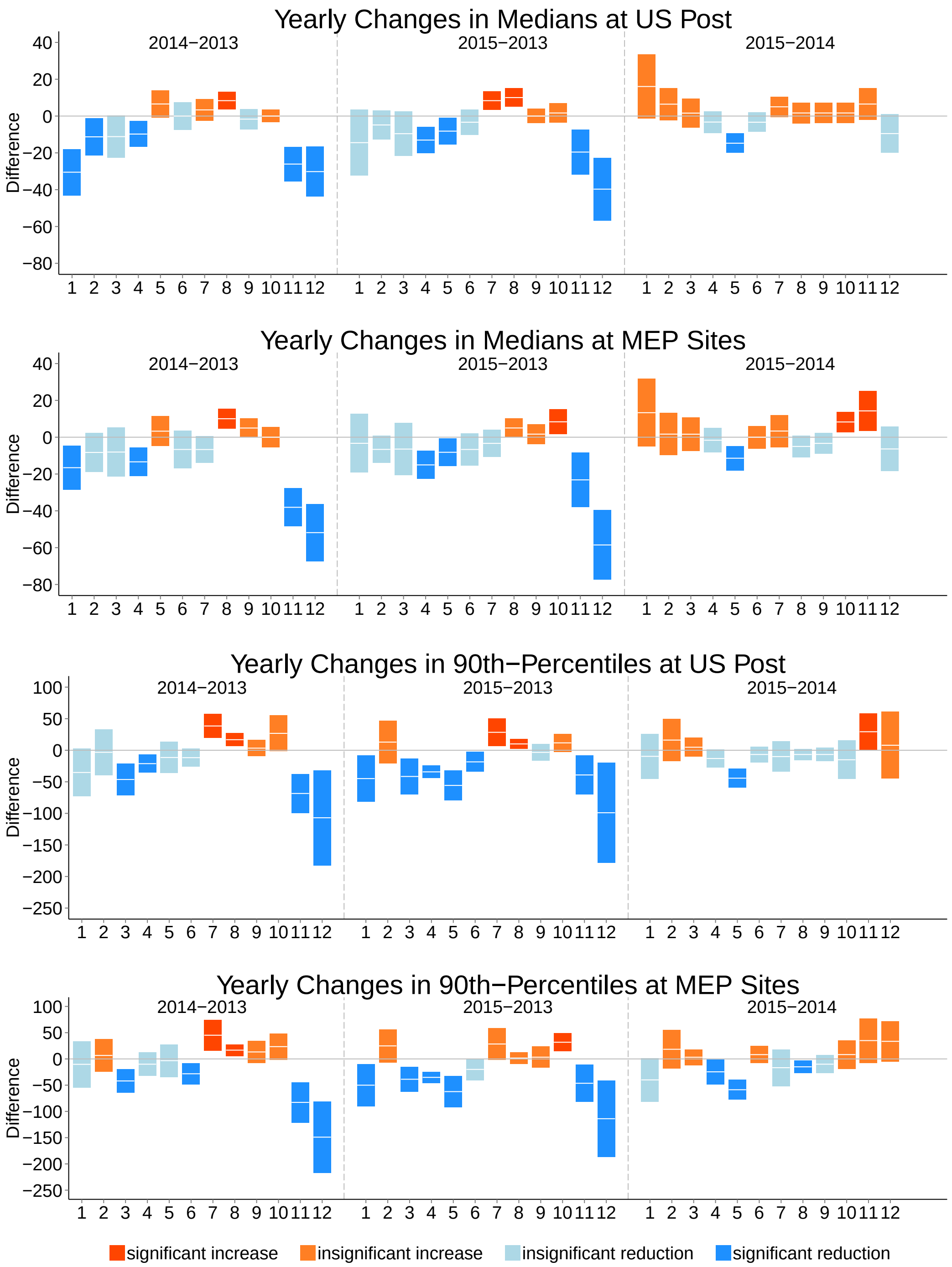

Yearly Changes in Medians at US Post
2014−2013
2015−2013
2015−2014
Difference
Yearly Changes in Medians at MEP Sites
2014−2013
2015−2013
2015−2014
Difference
Yearly Changes in 90th−Percentiles at US Post
2014−2013
2015−2013
2015−2014
Difference
Yearly Changes in 90th−Percentiles at MEP Sites
2014−2013
2015−2013
2015−2014
Difference
significant increase
insignificant increase
insignificant reduction
significant reduction

c: Guangzhou

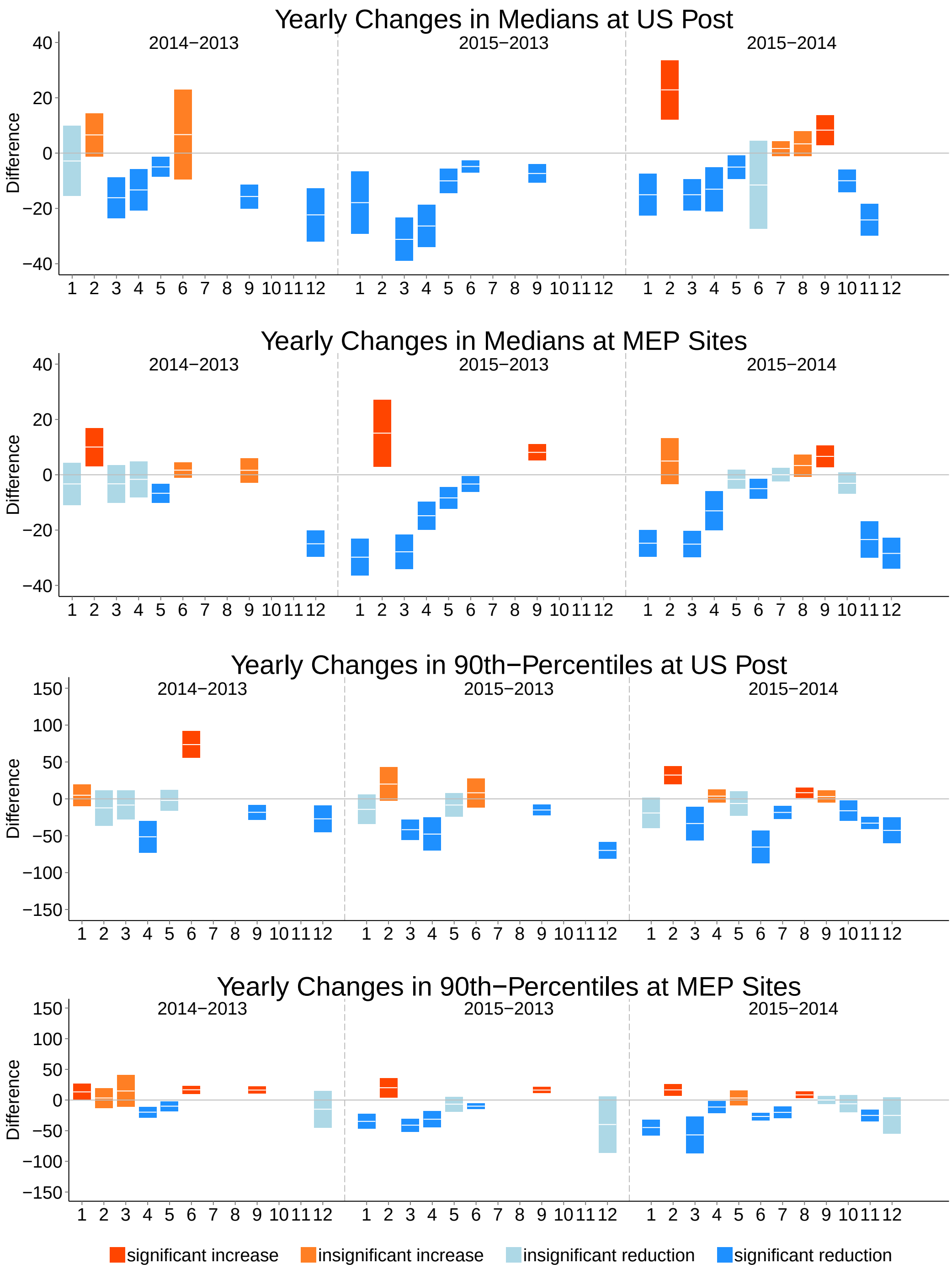
Yearly Changes in Medians at US Post
2014−2013
2015−2013
2015−2014
Difference
40
20
0
−20
−40
1 2 3 4 5 6 7 8 9 10 11 12
Yearly Changes in Medians at MEP Sites
Yearly Changes in 90th−Percentiles at US Post
150
100
50
−50
−100
−150
Yearly Changes in 90th−Percentiles at MEP Sites
significant increase
insignificant increase
insignificant reduction
significant reduction

d. Chengdu

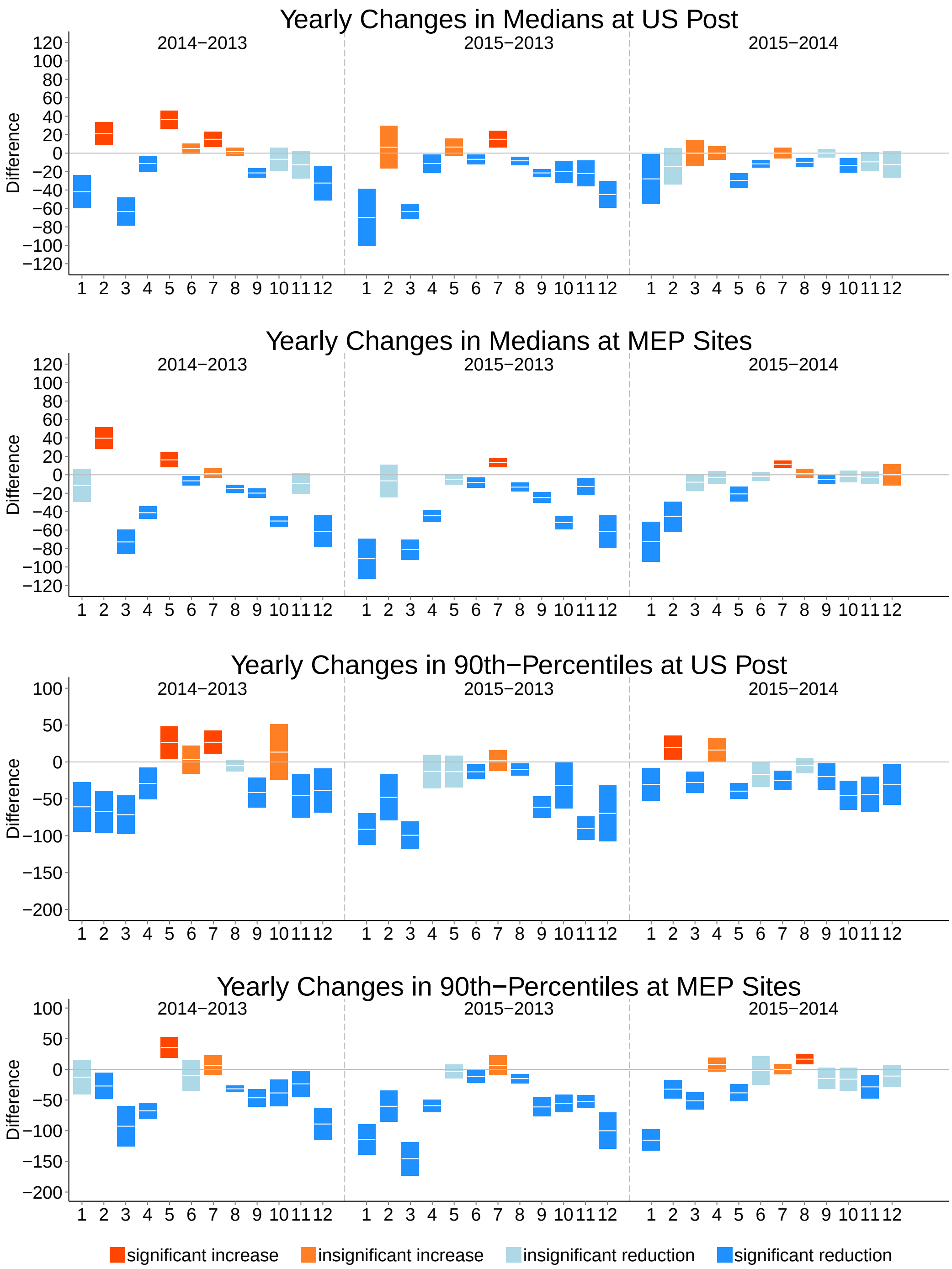
Yearly Changes in Medians at US Post
2014−2013
2015−2013
2015−2014
Difference
Yearly Changes in Medians at MEP Sites
Yearly Changes in 90th−Percentiles at US Post
Yearly Changes in 90th−Percentiles at MEP Sites
significant increase
insignificant increase
insignificant reduction
significant reduction

e. Shenyang

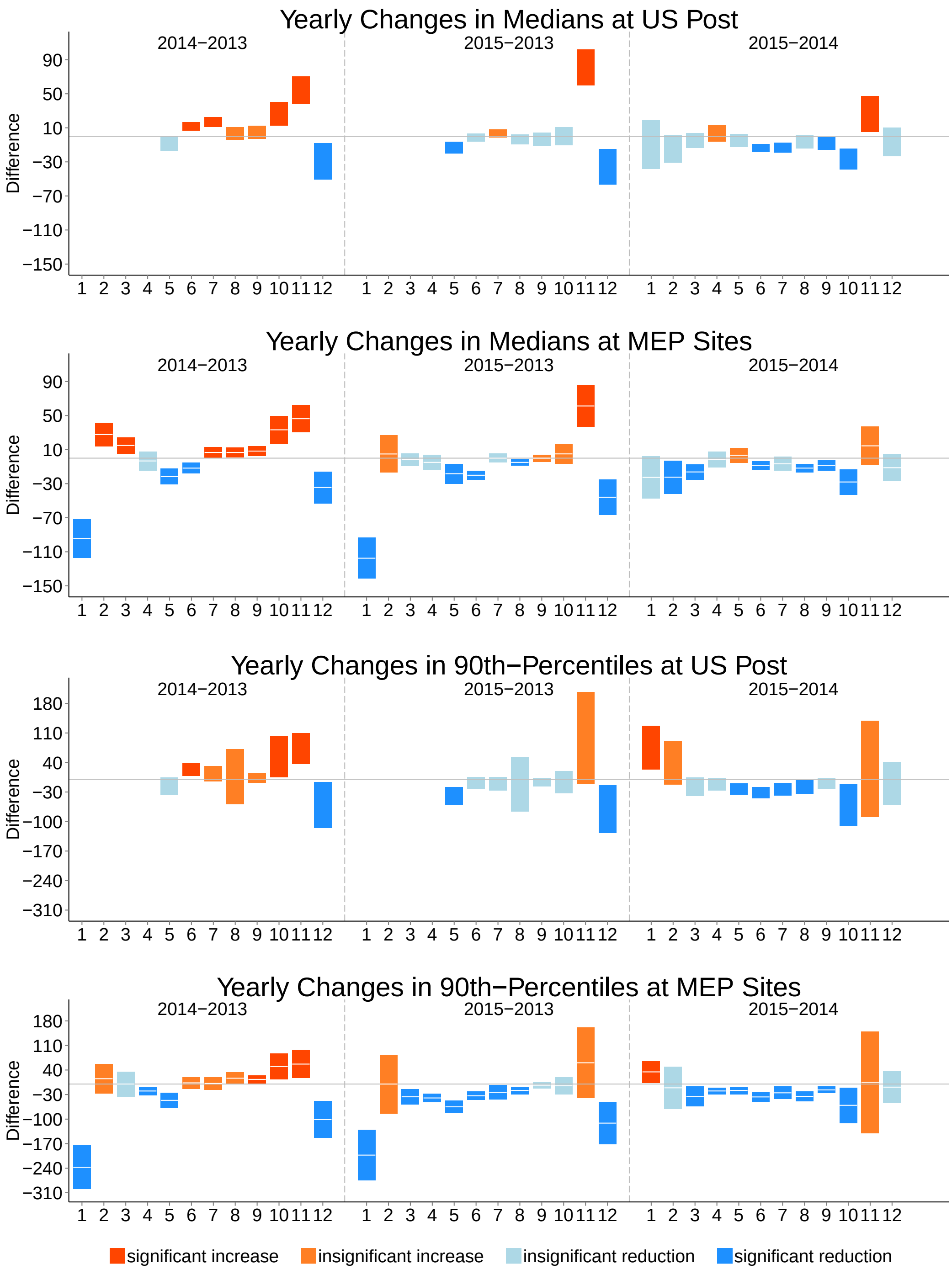

Figure S8. Yearly changes in the meteorologically adjusted medians and the 90th-percentiles in the US posts and the average of the MEP sites in five cities. The boxes are 1.96 times the standard deviations above and below the differences (white line). Significant increases (decreases) correspond to boxes which are entirely above (below) the horizontal line of zero; insignificant changes correspond to boxes which intercept the horizontal line.

Table S4. Pearson's Correlation coefficients in the three air quality metrics between the MEP sites and the US posts. The figures in the parentheses are the standard errors.

		2013	2014	2015	All
Beijing	Mean	0.95	0.97	0.99	0.96 (0.05)
	Median	0.70	0.93	0.96	0.93 (0.06)
	90th-Percentile	0.96	0.99	0.99	0.97 (0.04)
Shanghai	Mean	0.96	0.96	0.98	0.96 (0.05)
	Median	0.95	0.97	0.98	0.95 (0.05)
	90th-Percentile	0.98	0.95	0.96	0.97 (0.04)
Guangzhou	Mean	0.94	0.91	0.96	0.92 (0.07)
	Median	0.98	0.96	0.24	0.71 (0.14)
	90th-Percentile	0.95	0.76	0.66	0.72 (0.14)
Chengdu	Mean	0.97	0.97	0.99	0.96 (0.05)
	Median	0.97	0.97	0.99	0.96 (0.05)
	90th-Percentile	0.96	0.94	0.99	0.95 (0.05)
Shenyang	Mean	0.95	0.98	0.99	0.97 (0.04)
	Median	0.93	0.99	0.99	0.97 (0.05)
	90th-Percentile	0.98	0.98	0.99	0.97 (0.04)

Table S5. Pearson's correlation coefficients in the yearly changes of the three air quality metrics between the MEP sites and the US Posts. The figures in the parentheses are the standard errors.

		2014-2013	2015-2013	2015-2014	All
Beijing	Mean	0.96	0.81	0.95	0.91 (0.07)
	Median	0.94	0.87	0.87	0.89 (0.08)
	90th-Percentile	0.92	0.90	0.92	0.86 (0.09)
Shanghai	Mean	0.90	0.90	0.87	0.90 (0.07)
	Median	0.85	0.90	0.82	0.88 (0.08)
	90th-Percentile	0.96	0.99	0.85	0.95 (0.05)
Guangzhou	Mean	0.72	0.84	0.73	0.76 (0.13)
	Median	0.68	0.91	0.87	0.87 (0.10)
	90th-Percentile	0.62	0.76	0.72	0.69 (0.14)
Chengdu	Mean	0.74	0.93	0.58	0.80 (0.10)
	Median	0.77	0.93	0.66	0.81 (0.10)
	90th-Percentile	0.59	0.85	0.32	0.68 (0.12)
Shenyang	Mean	0.93	0.96	0.92	0.94 (0.06)
	Median	0.91	0.94	0.83	0.92 (0.07)
	90th-Percentile	0.95	0.94	0.92	0.91 (0.08)

Table S6. Regression coefficients and R^2 of the regression model: $MEP = \beta_0 + \beta_1 \times US + \epsilon$ on the adjusted metrics and their yearly changes. The figures in parentheses are the standard errors.

City	Metric	Adjustment			Yearly Changes		
		Intercept	Slope	R^2	Intercept	Slope	R^2
Beijing	Mean	16.32 (4.08)	0.81 (0.04)	0.91	3.99 (0.83)	0.83 (0.07)	0.83
	Median	12.67 (4.08)	0.79 (0.05)	0.86	-1.72 (1.89)	0.72 (0.06)	0.80
	90th-Percentile	23.90 (8.32)	0.90 (0.04)	0.95	7.96 (5.41)	0.81 (0.08)	0.74
Shanghai	Mean	7.97 (2.55)	0.92 (0.05)	0.92	-0.65 (1.08)	1.08 (0.09)	0.82
	Median	6.17 (2.37)	0.91 (0.05)	0.91	-0.74 (1.11)	1.11 (0.10)	0.78
	90th-Percentile	12.13 (4.74)	1.02 (0.04)	0.95	2.87 (1.21)	1.21 (0.06)	0.91
Guangzhou	Mean	8.88 (3.07)	0.81 (0.06)	0.85	-1.55 (1.97)	0.59 (0.10)	0.57
	Median	14.67 (6.65)	0.63 (0.12)	0.50	-1.16 (1.71)	0.77 (0.09)	0.75
	90th-Percentile	20.46 (12.20)	0.66 (0.12)	0.53	-3.43 (3.41)	0.50 (0.10)	0.47
Chengdu	Mean	-15.00 (5.06)	1.10 (0.06)	0.92	-5.82 (3.71)	1.07 (0.14)	0.64
	Median	-13.49 (4.92)	1.11 (0.06)	0.91	-7.00 (3.47)	1.07 (0.13)	0.66
	90th-Percentile	-16.68 (9.31)	1.05 (0.06)	0.90	-11.91 (6.91)	0.86 (0.16)	0.47
Shenyang	Mean	3.58 (3.22)	0.96 (0.04)	0.95	-5.44 (1.67)	1.01 (0.07)	0.88
	Median	3.95 (2.92)	0.92 (0.04)	0.94	-5.78 (1.64)	0.86 (0.07)	0.84
	90th-Percentile	4.31 (7.16)	0.98 (0.04)	0.94	-15.13 (2.98)	0.93 (0.08)	0.84

Text S5. Heating Effect

In this section, we provide detailed numeric results about the heating effects for the five cities, respectively. In Table S7, the original means of the raw data and the adjusted means for each site are reported. One can see a clear rise (reduction) of the adjusted values in Novembers (Marches) in Beijing, around the time the heating season starts (ends). As for Shenyang, the rises of the adjusted values in November are not significant due to biomass burning. But the results in March are similar to those of Beijing. This demonstrates the necessity to adjust for weather conditions when one is making an assessment of pollution levels over years. Table S8 summarizes the testing results about the heating effect for the five cities.

Table S7. Original average and adjusted average of $PM_{2.5}$ concentration. The figures in parentheses are the standard errors. Percentage in Heating effect means the ratio of the difference between the adjusted Heating average and the adjusted Non-heating average to the adjusted Non-heating average. P value is about the one sided hypothesis H_0: no "heating effect" v.s. H_1: there is a "heating effect". In the column "Bonferroni" one means that we reject the hypothesis if we use the Bonferroni method for the multiple testing at level 0.05.

(a) Beijing November

		Original		Adjusted		Heating effect		
Site	Year	Non-heating	Heating	Non-heating	Heating	Percentage(%)	P value	Bonferroni
US Embassy	2013	115.25	69.11	106.03 (7.10)	135.77 (13.90)	28.05	0.021	0
	2014	50.12	152.74	52.16 (5.35)	135.85 (10.75)	160.44	<0.001	1
	2015	125.61	124.13	66.13 (6.57)	210.33 (33.54)	218.07	<0.001	1
Nongzhanguan	2013	107.18	62.33	97.75 (7.07)	135.35 (15.06)	38.47	0.007	1
	2014	51.03	155.16	57.72 (5.49)	137.37 (10.75)	138.00	<0.001	1
	2015	130.76	130.65	72.29 (7.37)	225.08 (34.05)	211.34	<0.001	1
Dongsihuan	2013	107.77	62.85	102.95 (7.07)	113.26 (11.17)	10.01	0.186	0
	2014	57.45	182.56	64.17 (5.54)	158.59 (11.46)	147.12	<0.001	1
Dongsi	2013	104.44	64.20	93.97 (6.44)	136.42 (13.97)	45.17	0.002	1
	2014	38.49	119.59	40.67 (3.9)	101.03 (8.59)	148.43	<0.001	1
	2015	126.60	127.75	72.15 (5.76)	244.8 (48.73)	239.28	<0.001	1

(b) Beijing March

		Original		Adjusted		Heating effect		
Site	Year	Heating	Non-heating	Heating	Non-heating	Percentage(%)	P value	Bonferroni
US Embassy	2013	164.44	94.76	131.23 (10.32)	79.16 (6.13)	65.78	<0.001	1
	2014	95.03	124.99	126.25 (9.78)	92.72 (7.82)	36.16	0.002	1
	2015	83.44	95.50	101.54 (7.39)	69.4 (7.65)	46.32	<0.001	1
Nongzhanguan	2013	143.63	83.11	117.14 (8.57)	72.49 (5.03)	61.58	<0.001	1
	2014	85.14	113.24	117.17 (8.68)	87.92 (8.91)	33.27	0.005	1
	2015	86.39	101.91	113.03 (8.22)	72.37 (6.66)	56.19	<0.001	1
Dongsihuan	2013	173.38	89.38	130.86 (9.75)	76.49 (5.49)	71.09	<0.001	1
	2014	83.95	117.64	115.14 (8.75)	85.98 (6.97)	33.91	0.002	1
	2015	98.97	107.54	122.95 (8.34)	78.84 (7.78)	55.95	<0.001	1
Dongsi	2013	145.31	84.88	119.36 (8.81)	73.01 (5.22)	63.49	<0.001	1
	2014	82.39	115.25	109.64 (8.42)	83.56 (7.62)	31.22	0.006	1
	2015	92.35	95.58	124.37 (9.32)	68.06 (6.82)	82.73	<0.001	1

(c) Shenyang November

Site	Year	Original		Adjusted		Heating effect		
		Non-heating	Heating	Non-heating	Heating	Percentage(%)	P value	Bonferroni
US Consulate	2013	111.65	74.67	78.69 (6.30)	78.52 (4.84)	-0.21	0.509	0
	2014	146.21	103.92	159.63 (18.07)	166.61 (19.39)	4.37	0.390	0
	2015	84.53	199.82	87.27 (7.07)	164.08 (16.26)	88.01	<0.001	1
Taiyuanjie	2013	113.25	81.10	89.93 (8.87)	75.9 (4.94)	-15.60	0.909	0
	2014	161.13	105.22	188.48 (21.53)	163.06 (16.99)	-13.49	0.855	0
	2015	81.22	198.52	88.47 (7.55)	154.35 (18.56)	74.47	<0.001	1
Xiaoheyan	2013	110.17	76.66	90.78 (7.40)	72.54 (4.49)	-20.09	0.984	0
	2014	149.47	96.89	158.52 (22.8)	167.19 (26.51)	5.47	0.396	0
	2015	86.72	214.78	99.47 (8.81)	165.75 (20.70)	66.62	0.001	1

(d) Shenyang March

Site	Year	Original		Adjusted		Heating effect		
		Heating	Non-heating	Heating	Non-heating	Percentage(%)	P value	Bonferroni
US Consulate	2014	94.66	67.33	82.04 (5.79)	61.89 (3.63)	32.55	0.001	1
	2015	91.98	69.75	88.13 (4.45)	67.25 (2.38)	31.05	<0.001	1
Taiyuanjie	2013	75.01	60.89	90.33 (9.16)	62.38 (4.77)	44.81	0.001	1
	2014	105.09	79.31	96.02 (6.98)	67.44 (3.88)	42.37	<0.001	1
	2015	94.99	73.66	86.3 (4.98)	69.5 (3.08)	24.18	0.001	1
Xiaoheyan	2013	65.53	54.74	80.38 (7.63)	49.73 (3.59)	61.62	<0.001	1
	2014	97.71	72.76	82.82 (5.29)	62.28 (3.74)	32.98	<0.001	1
	2015	80.12	65.61	72.81 (4.11)	61.45 (2.37)	18.49	0.008	1

(e) Shanghai November

Site	Year	Original		Adjusted		Heating effect		
		Non-heating	Heating	Non-heating	Heating	Percentage(%)	P value	Bonferroni
US Consulate	2013	69.27	87.78	81.5 (8.10)	81.75 (4.18)	0.32	0.489	0
	2014	57.34	50.18	49.89 (4.20)	50.65 (4.04)	1.53	0.446	0
	2015	62.26	51.45	51.36 (3.63)	59.59 (6.75)	16.04	0.122	0
Jingan	2013	68.03	89.04	89.53 (12.10)	87.56 (5.41)	-2.19	0.558	0
	2014	57.63	48.55	47.73 (4.54)	46.55 (3.74)	-2.47	0.585	0
	2015	65.10	55.28	53.87 (5.07)	62.12 (7.50)	15.32	0.165	0
Xuhui	2013	73.61	100.67	86.55 (9.03)	99.18 (6.37)	14.58	0.134	0
	2014	60.65	49.21	53.31 (4.68)	48.3 (3.91)	-9.39	0.804	0
	2015	64.28	51.76	51.58 (4.70)	59.96 (7.29)	16.25	0.155	0

(f) Shanghai March

Site	Year	Original		Adjusted		Heating effect		
		Heating	Non-heating	Heating	Non-heating	Percentage(%)	P value	Bonferroni
US Consulate	2013	75.41	55.22	80.85 (6.57)	48.68 (2.41)	66.07	<0.001	1
	2014	49.17	59.44	46.24 (2.91)	54.8 (3.12)	-15.61	0.973	0
	2015	52.91	48.28	62.94 (4.63)	43.52 (2.73)	44.61	<0.001	1
Jingan	2013	78.72	51.74	79.11 (7.27)	46.04 (2.45)	71.83	<0.001	1
	2014	48.22	60.67	44.61 (3.78)	50.56 (3.92)	-11.77	0.849	0
	2015	54.91	51.80	54.76 (4.42)	40.23 (3.28)	36.13	0.004	1
Xuhui	2013	78.95	49.53	83.55 (6.83)	45.31 (2.28)	84.38	<0.001	1
	2014	52.51	67.07	46.97 (3.18)	61.18 (3.83)	-23.23	0.997	0
	2015	54.59	50.12	53.31 (4.54)	44.04 (3.07)	21.03	0.047	0

(g) Guangzhou November

Site	Year	Original: Non-heating	Original: Heating	Adjusted: Non-heating	Adjusted: Heating	Heating effect: Percentage(%)	Heating effect: P value	Heating effect: Bonferroni
US Consulate	2013	58.32	54.58	53.22 (2.96)	68.98 (4.20)	29.62	0.001	1
	2014	44.29	61.74	47.21 (3.22)	61.96 (1.83)	31.23	<0.001	1
	2015	35.86	40.99	29.85 (2.48)	32.12 (2.13)	7.59	0.245	0
5th Middle School	2014	44.27	60.22	44.97 (3.02)	61.9 (1.80)	37.63	<0.001	1
	2015	38.89	41.42	32.08 (2.38)	37.27 (2.64)	16.18	0.074	0
City Station	2014	40.21	53.46	43.71 (3.01)	53.14 (1.60)	21.58	0.005	1
	2015	32.91	36.18	28.86 (2.45)	34.08 (2.54)	18.08	0.072	0

(h) Guangzhou March

Site	Year	Original: Heating	Original: Non-heating	Adjusted: Heating	Adjusted: Non-heating	Heating effect: Percentage(%)	Heating effect: P value	Heating effect: Bonferroni
US Consulate	2013	79.83	57.72	74.01 (4.75)	53.36 (6.19)	38.69	0.007	1
	2014	51.16	60.23	50.68 (8.27)	55.58 (3.10)	-8.81	0.715	0
	2015	44.18	38.51	44.54 (4.68)	36.67 (1.78)	21.47	0.058	0
5th Middle School	2013	74.13	49.93	69.51 (3.96)	44.53 (4.06)	56.11	<0.001	1
	2014	54.88	68.68	57.98 (7.02)	65.9 (2.96)	-12.01	0.849	0
	2015	37.39	37.55	39.05 (4.12)	36.96 (1.31)	5.66	0.316	0
City Station	2013	76.25	50.74	70.33 (3.67)	53.39 (4.99)	31.74	0.005	1
	2014	54.97	67.26	65.09 (10.28)	61.63 (2.49)	5.61	0.371	0
	2015	31.97	33.33	32.6 (4.08)	33.19 (1.20)	-1.79	0.556	0

(i) Chengdu November

Site	Year	Original: Non-heating	Original: Heating	Adjusted: Non-heating	Adjusted: Heating	Heating effect: Percentage(%)	Heating effect: P value	Heating effect: Bonferroni
US Consulate	2013	70.32	129.81	69.59 (3.11)	140.86 (7.76)	102.40	<0.001	1
	2014	64.47	73.61	79.17 (7.62)	73.21 (3.37)	-7.53	0.788	0
	2015	58.04	61.87	43.62 (5.40)	59 (2.69)	35.27	0.002	1
Caotangsi	2013	40.23	89.17	40.87 (1.85)	95.8 (4.53)	134.38	<0.001	1
	2014	53.04	57.13	66.78 (6.52)	58.36 (2.48)	-12.60	0.918	0
	2015	48.90	51.83	38.04 (4.92)	48.64 (2.56)	27.84	0.023	0
Shahepu	2013	46.70	90.72	46.73 (2.35)	99.19 (5.82)	112.28	<0.001	1
	2014	51.47	57.49	60.6 (6.05)	60.15 (2.88)	-0.75	0.530	0
	2015	43.24	49.04	33.1 (4.51)	44.84 (2.59)	35.47	0.007	1

(j) Chengdu March

Site	Year	Original: Heating	Original: Non-heating	Adjusted: Heating	Adjusted: Non-heating	Heating effect: Percentage(%)	Heating effect: P value	Heating effect: Bonferroni
US Consulate	2013	152.98	115.80	150.48 (5.18)	122.79 (6.94)	22.55	<0.001	1
	2014	62.66	106.05	77.17 (4.30)	88.2 (6.33)	-12.51	0.903	0
	2015	82.95	77.68	83.08 (3.00)	57.55 (3.53)	44.37	<0.001	1
Caotangsi	2013	177.45	102.79	175.66 (6.64)	95.14 (10.71)	84.64	<0.001	1
	2014	63.01	104.77	74.59 (2.99)	86.44 (6.23)	-13.71	0.947	0
	2015	67.32	60.98	70.33 (3.36)	43.94 (3.59)	60.05	<0.001	1
Shahepu	2013	172.87	103.66	162.62 (5.33)	94.73 (9.00)	71.67	<0.001	1
	2014	62.29	99.60	70.79 (5.14)	87.02 (5.79)	-18.64	0.977	0
	2015	69.69	60.05	75.91 (2.56)	37.54 (2.97)	102.23	<0.001	1

Table S8. Number of the rejected hypothesis for testing H_0: no "heating effect" v.s. H_1: there is a "heating effect" at the level 5%. 'Total" – the total number of the site and year combinations in a city; "Site Specific" – number of rejections based on the single test at each site and year combination; "Bonferroni" – number of rejections based on the Bonferroni correction.

		Beijing	Shenyang	Shanghai	Guangzhou	Chengdu
March	Total	12	8	9	9	9
	Site Specific	12	8	6	3	6
	Bonferroni	12	8	5	3	6
November	Total	11	9	9	7	9
	Site Specific	10	3	0	4	6
	Bonferroni	9	3	0	4	5

Text S6. Geography, Climate and Economy of the Five Cities

Beijing is situated at the north-west corner of North China Plain (NCP) with Taihang Mountain to the west and Yan Mountain to the north. The mountainous region to the west and the north has much lower population density and less industry activities, and hence pollution emissions. However, the region south and east of Beijing on the NCP is densely populated with heavy industries that consume enormous amount of coal and other fossil fuels, which severely influence Beijing's air quality. Here, NCP refers only to Beijing, Tianjing and Hebei province combined, excluding the north parts of Hebei and Shandong. Beijing has a semi-humid monsoon-influenced continental climate. It is generally dry except in the summer when most of the precipitation happens. The population in Beijing was 21.5 million in 2014 and that in NCP was 111 million. Hereafter, our data on energy consumption and economic are from [*National Bureau of Statistics*, 2015]. The GDP of NCP in 2014 was 6647.45 billion Renminbi (RMB), with the shares of the primary, manufacturing (secondary) and service (tertiary) sectors being 5.7%, 41.06% and 53.21% of the gross domestic product, respectively.

Shanghai is located 30 km to the East China Sea, and is in the center east region of the Yangtze River Delta (YRD). Here, YRD refers to Shanghai, Jiangsun and Zhejiang provinces combined. It has the subtropical monsoon climate with distinct four seasons. The population in Shanghai was 24 millions in 2014, and that in the YRD was 158 million. YRD is quite flat in its central and the northern parts with mountains only appeared in the southern part in Zhejiang province. Shanghai sits in a quite open plain with the nearest mountain range (Tianmu Mountain) 220 km away in the south-west. Most of the industrial activities take place in the regions west, northwest and southwest of Shanghai. Shanghai has the major commercial and financial centers of China. YRD commands the leading position in both economic outputs and energy consumption in China, as reflected in both the energy and the GDP statistics conveyed in Figure S9 and Figure S10, as well as the energy usage per unit land area (Table S10). YRD is one of the most economically vibrant and efficient region in China with the highest GDP, 12880.28 billion RMB in 2014, among the five regions. Moreover, the composition of its econmy was 4.30% primary, 45.32% secondary and 50.38% service.

Guangzhou is situated in the northern end of the Pearl River Delta (PRD) on the bank of Pearl River in Guangdong province. Guangdong belongs to South China region, facing the South China Sea. Guangzhou's population was 13.08 million in 2014, and that in Guangdong was 107.24 million. It has a similar climate to Shanghai: subtropical monsoon climate, except its temperature is warmer, especially in winter. Guangzhou is mostly flat except Jiulong Mountain slants in from the Northeast, whose peak (Tiantang Peak, elevation 1210 meters) is 200 km away from the city. Guangzhou is about 55 km to the mouth of the Pearl River, and 125 km to the South China Sea in the south. The main industrial area in Guangdong is to the south of Guangzhou in PRD. Guangdong's economic structure at 2014 was 4.7% primary, 46.2% manufacturing and 49.1% service.

Chengdu is located at the west part of the Sichuan Basin at the center of the Chengdu plain with quite high mountains to its west and north. The hypsography of Chengdu slants gradually from the mountainous northwest to Chengdu Plain in the east and southeast. Chengdu Plain has the lowest altitude in the Sichuan Basin, and is known for its fertile land, rich culture and cuisine. Chengdu's climate is subtropical humid monsoon climate. The topography of Chengdu determines that it is lack of strong wind as compared to other four metropolises. In our analysis on the energy consumption and economic output, we combine Sichuan and Chongqing together as one area. Chongqing was separated from Sichuan in 1997 to become a provincial level city. Manufacturing (secondary sector of economy) occupies the largest share (49%) among the three main economic sectors in Sichuan and Chongqing, followed by the service (40%) and the primary (11%) sectors.

Shenyang is located in the Liao River Plain at central Liaoning Province in Northeast China. Shenyang's population was 7.2 million in 2013, and that in Liaoning was 44 million in 2014. Shenyang has the sub-humid temperate continental climate, with the coldest winter among the five cities. Unlike Beijing and Chengdu, and similar to Guangzhou and Shanghai, Shenyang sits in a relatively open plain which is favorable for the diffusion of pollutants. Liaoning along with the Northeast region used to be the center of heavy industries in China. However, its share of the heavy industrial related GDP has been declining since 1990s as many state owned enterprises bankrupted or being transformed. In comparison, NCP (the region south and east of Beijing) has taken more share of the heavy industrial from Liaoning and Northeast China region. The GDP of Liaoning was 2862.66 billion in 2014. As a traditional industrial region in China prior to the economic opening up in the 1980s, the secondary sector (manufacturing) was still the largest at 50.25% of the GPD in 2014, while the agriculture and primary industry's share of economy was 7.9% and the service sector was 41.77%.

As far as the topographical situation is concerned, Beijing and Chengdu have the worst condition for diffusion of pollutants since Beijing is hemmed in by mountains from two sides, and Chengdu is at the western edge of Sichuan Basin. Also Guangzhou is penetrated in by a mountain range from the northeast, but it is much more openly laid than Beijing and Chengdu, and is quite close to the sea. Shanghai and Shenyang lay in relatively open terrain. Shanghai has the best geographical conditions and is the most close to the sea.

Text S7. Energy Consumption and GDP

In this section, we provide summary statistics of energy consumption and GDP for the regions where the five cities are located at. The data are available up to 2014. Both streams of data are administrated by China's National Bureau of Statistics.

In term of energy consumption, YRD (Shanghai) was the top user of coal, diesel and petrol. These reflected YRD being the number one GDP producer among the five regions as shown in Figure S10, which almost doubled the GDP of the 2nd ranked PRD (Guangzhou) and the 3rd ranked NCP (Beijing). NCP was ranked the second for coal. The coal usage in YRD and NCP were much larger than those of the other three regions. PRD (Guangzhou) ranked second in diesel consumption. Liaoning and Sichuan-Chongqing regions were the bottom two users in diesel and petrol, and were at a par with PRD for coal.

The above comparisons are based on the absolute energy usage, which may be misleading as it does not take into account of the land area of the regions. We compute two energy intensities: one standardized by the land area and the other by the total GDP of the regions. Under the measure of energy intensity by area (Figure 6 and Table S10), YRD had the highest intensity in all the three forms of energy and Sichuan-Chongqing had the least intensity. NCP had the second highest intensity in coal.

If standardized by GDP (Table S11), YRD was at the bottom of the rank in diesel, and the second lowest in coal and petrol, and Liaoning had the highest intensity in coal, diesel and petrol, and Sichuan-Chongqing region moved up to the third place in coal, and the second places in diesel and petrol. NCP ranked the second in coal. These figures show that YRD (Shanghai) has the most energy efficient economy, followed by Guangdong. Liaoning, Sichuan-Chongqing and NCP are lagged behind these two regions, indicating the economies of these three regions are more energy intensive. These are related to the economic structures of these regions with the YRD and PRD regions have more share of light manufacturing and service industries, whileas those in the NCP and Liaoning are much driven by the heavy industries and thus less energy efficiency.

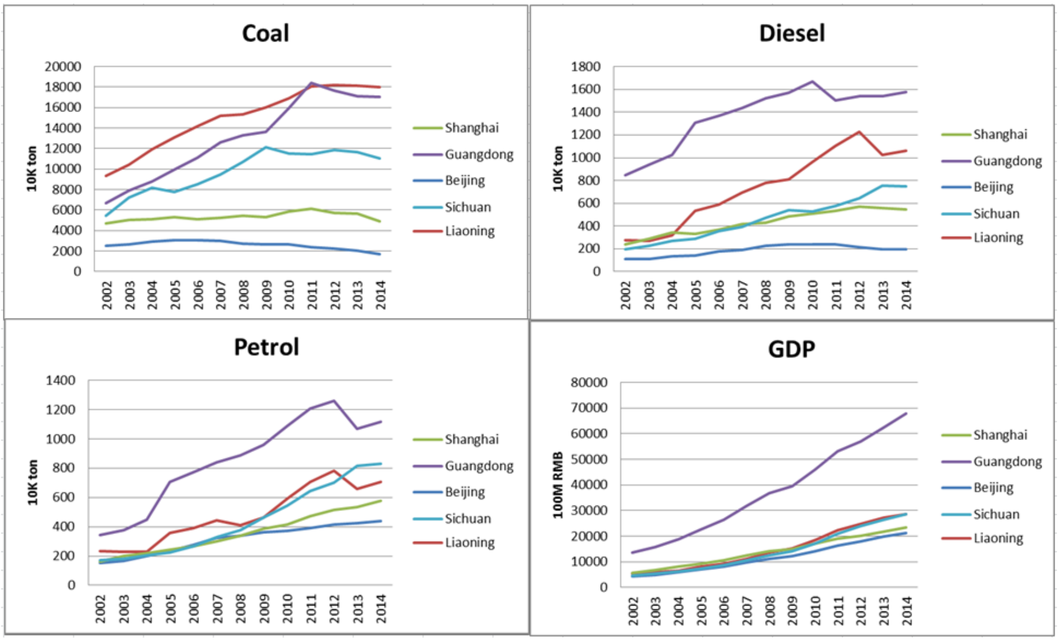

Figure S9. Energy consumption and GDP of the five cities/Provinces. Data source: National Bureau of Statistics of China.

Table S9. Area of Five Cities/Regions. Unit: 10000 square kilometers. SC-CQ abbreviates for Sichuan and Chongqing.

City	Beijing	Shenyang	Shanghai	Guangzhou	Chengdu
Area	1.64	1.30	0.63	0.74	1.24
Region	NCP	Liaoning	YRD	Guangdong	SC-CQ
Area	21.63	14.80	21.07	17.98	56.84

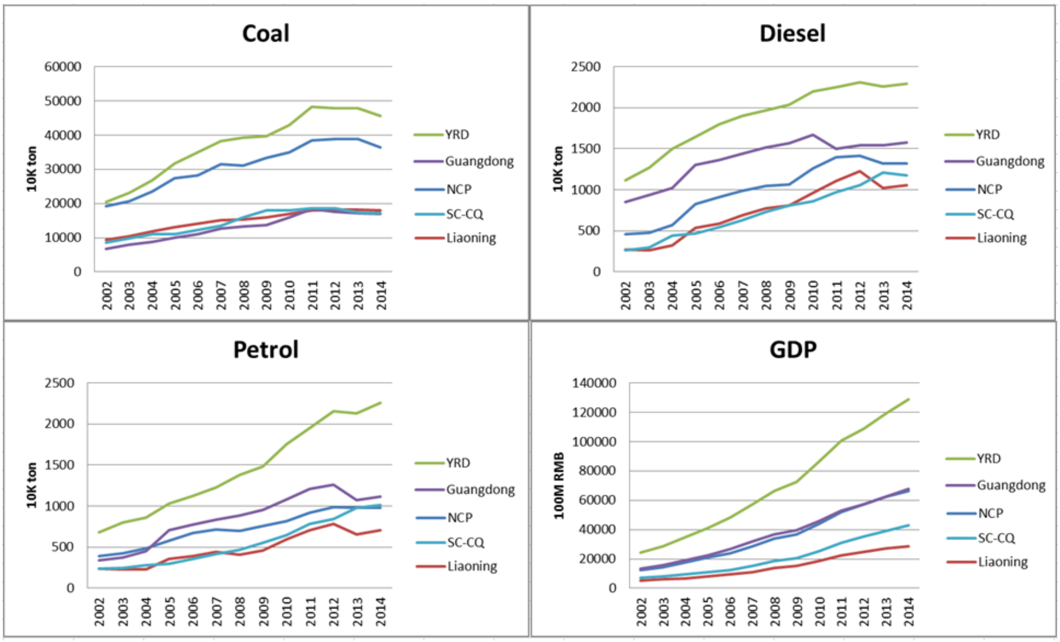

Figure S10. Energy Consumption and GDP of the five regions where the five cities are. SC-CQ abbreviates for Sichuan and Chongqing. Data source: National Bureau of Statistics of China.

Table S10. Intensity of energy consumption per unit area (10^4 ton per 10000 square kilometers) of the five regions. SC-CQ abbreviates for Sichuan and Chongqing.

		2002	2003	2004	2005	2006	2007	2008	2009	2010	2011	2012	2013	2014
Coal/Area	NCP	883.93	954.45	1082.96	1262.10	1298.82	1448.43	1433.66	1533.16	1607.10	1768.88	1792.22	1801.26	1682.82
	Liaoning	632.09	706.34	807.09	883.09	960.22	1028.67	1036.94	1083.28	1142.46	1219.86	1231.01	1225.19	1216.37
	YRD	966.59	1097.91	1270.92	1508.49	1656.63	1814.69	1862.44	1878.71	2037.30	2291.50	2270.48	2268.08	2165.77
	Guangdong	369.80	439.95	488.89	552.97	618.80	700.44	739.61	759.02	888.97	1025.53	980.76	951.43	946.26
	SC-CQ	149.81	174.18	195.16	195.76	215.82	238.02	281.49	315.43	315.22	327.99	327.62	307.41	301.57
Diesel/Area	NCP	21.29	22.01	26.17	37.88	41.85	45.38	48.28	49.05	58.14	64.36	65.16	60.99	61.01
	Liaoning	18.46	18.09	21.74	36.11	39.71	46.87	52.60	54.76	65.13	74.63	82.80	69.03	71.63
	YRD	53.07	60.38	71.02	78.21	85.46	90.15	93.59	96.64	104.19	106.82	109.70	107.01	108.90
	Guangdong	47.17	52.05	56.93	72.67	76.06	79.99	84.48	87.20	92.80	83.46	85.79	85.57	87.61
	SC-CQ	4.67	5.28	7.73	8.23	9.52	11.05	12.87	14.29	15.19	17.14	18.53	21.29	20.66
Petrol/Area	NCP	18.22	19.82	22.51	26.63	30.97	33.01	32.40	34.98	37.70	42.45	45.68	45.46	45.40
	Liaoning	15.95	15.40	15.49	24.13	26.59	29.87	27.74	31.35	40.08	47.74	52.76	44.52	47.62
	YRD	32.51	38.14	41.00	48.93	53.30	58.30	65.38	70.37	83.15	92.45	102.44	101.10	107.36
	Guangdong	19.16	20.86	24.89	39.28	42.90	46.59	49.33	53.24	60.41	67.16	70.05	59.54	62.23
	SC-CQ	4.17	4.35	4.93	5.31	6.26	7.33	8.31	9.74	11.34	13.85	14.86	17.24	17.80

Table S11. Energy consumption per unit GDP (10^4 ton per 10^8 RMB) of the five regions. SC-CQ abbreviates for Sichuan and Chongqing.

		2002	2003	2004	2005	2006	2007	2008	2009	2010	2011	2012	2013	2014
	NCP	1.538	1.429	1.335	1.312	1.173	1.096	0.920	0.902	0.798	0.738	0.679	0.622	0.548
	Liaoning	1.714	1.742	1.790	1.624	1.527	1.364	1.123	1.054	0.916	0.812	0.733	0.666	0.629
Coal/GDP	YRD	0.836	0.802	0.771	0.770	0.727	0.668	0.590	0.546	0.497	0.480	0.439	0.400	0.354
	Guangdong	0.492	0.499	0.466	0.441	0.418	0.396	0.361	0.346	0.347	0.347	0.309	0.274	0.251
	SC-CQ	1.224	1.255	1.178	1.025	0.974	0.888	0.870	0.867	0.714	0.601	0.528	0.446	0.401
	NCP	0.037	0.033	0.032	0.039	0.038	0.034	0.031	0.029	0.029	0.027	0.025	0.021	0.020
	Liaoning	0.050	0.045	0.048	0.066	0.063	0.062	0.057	0.053	0.052	0.050	0.049	0.038	0.037
Diesel/GDP	YRD	0.046	0.044	0.043	0.040	0.037	0.033	0.030	0.028	0.025	0.022	0.021	0.019	0.018
	Guangdong	0.063	0.059	0.054	0.058	0.051	0.045	0.041	0.040	0.036	0.028	0.027	0.025	0.023
	SC-CQ	0.038	0.038	0.047	0.043	0.043	0.041	0.040	0.039	0.034	0.031	0.030	0.031	0.027
	NCP	0.032	0.030	0.028	0.028	0.028	0.025	0.021	0.021	0.019	0.018	0.017	0.016	0.015
	Liaoning	0.043	0.038	0.034	0.044	0.042	0.040	0.030	0.031	0.032	0.032	0.031	0.024	0.025
Petrol/GDP	YRD	0.028	0.028	0.025	0.025	0.023	0.021	0.021	0.020	0.020	0.019	0.020	0.018	0.018
	Guangdong	0.026	0.024	0.024	0.031	0.029	0.026	0.024	0.024	0.024	0.023	0.022	0.017	0.017
	SC-CQ	0.034	0.031	0.030	0.028	0.028	0.027	0.026	0.027	0.026	0.025	0.024	0.025	0.024